NACA

RESEARCH MEMORANDUM

DIFFUSION FACTOR FOR ESTIMATING LOSSES AND LIMITING BLADE LOADINGS IN AXIAL-FLOW-COMPRESSOR BLADE ELEMENTS

By Seymour Lieblein, Francis C. Schwenk
and Robert L. Broderick

Lewis Flight Propulsion Laboratory
Cleveland, Ohio

NATIONAL ADVISORY COMMITTEE
FOR AERONAUTICS

WASHINGTON

June 8, 1953

NATIONAL ADVISORY COMMITTEE FOR AERONAUTICS

RESEARCH MEMORANDUM

DIFFUSION FACTOR FOR ESTIMATING LOSSES AND LIMITING BLADE LOADINGS IN AXIAL-FLOW-COMPRESSOR BLADE ELEMENTS

By Seymour Lieblein, Francis C. Schwenk, and
Robert L. Broderick

SUMMARY

DESIGN

A simplified limiting-blade-loading parameter for axial-flow-compressor blade elements was derived from the application of a separation criterion used in two-dimensional boundary-layer theory to a typical suction-surface velocity distribution of a compressor blade element at design angle of attack. The derived limiting diffusion factor comprised a term involving the relative velocity ratio across the blade and a term proportional to the circulation about the element, both of which can be evaluated readily from the design velocity diagram.

A correlation was made for the data for NACA 65-series compressor blade sections in low-speed two-dimensional cascade between blade-element loss at design angle of attack and several commonly used and proposed blade-loading parameters. The derived diffusion factor constituted a satisfactory limiting-loading criterion for these data. Total-pressure loss coefficient at design angle of attack increased slightly with diffusion factor up to a value of about 0.6, after which a sharp rise in loss was observed.

Loss coefficient and diffusion correlations were also made for a large number of conventional experimental axial-flow single-stage compressor rotors and stators. For the hub- and mean-radius regions of the rotors and for the hub, mean, and tip regions of the stators, no consistent variation of loss coefficient with diffusion factor was observed in the low-loss range up to values of diffusion factor of about 0.55 to 0.65, the extent of the available data. For the tip region of the rotors, however, there was a very marked and practically linear variation of loss coefficient with diffusion factor, with resulting blade-element efficiencies less than 0.90 for values of diffusion factor greater than about 0.45. Further verification of the limiting relative inlet Mach number of about 0.70 to 0.75 for subcritical values of diffusion factor was indicated for rotor and stator blades of NACA 65-series profile shapes with about 10 percent maximum thickness ratios.

INTRODUCTION

One of the principal limitations and losses in the flow across axial-flow-compressor blade rows is due to the separation of the friction boundary layers on the suction surfaces of the blades. In airfoil theory, the measure of this limiting blade loading or diffusion was satisfactorily established by the variation of the lift coefficient of the section. (Lift coefficient is defined as lift force per unit blade area divided by inlet or vector-mean dynamic head.) The use of lift coefficient as a measure of loss variation and limiting loading was not, however, generally successful in compressor design application. Furthermore, the use of lift coefficient for the general compressor case of compressible flow with unequal axial velocities at blade-element inlet and outlet presents a difficulty in establishing a significant vector-mean condition. Consequently, various other loading parameters were tried in compressor design with varying degrees of success. These parameters were lift coefficients based on inlet or outlet conditions, solidity multiplied by lift coefficient, ratio of change in tangential velocity to axial velocity, ratio of axial velocity to tip speed, and so forth.

In reference 1, Wislicenus proposes an approximate stalling coefficient for axial-flow blades derived from considerations of the stalling suction-surface pressure distribution of isolated airfoils in incompressible flow. The coefficient is developed in terms of vector-mean velocity and indicates that the stalling pressure rise is a function of the sum of the conventional lift coefficient and the over-all change in free-stream velocity across the blade row. Howell, in reference 2, develops an approximate loading parameter for compressor blade elements from the application of a separation criterion used in boundary-layer theory. This parameter involves the product of the mean-velocity lift coefficient and a function of the over-all velocity ratio. No extensive experimental investigations of these various loading parameters have as yet appeared.

A similar approach to the development of an improved separation criterion for axial-flow blade elements was made at the NACA Lewis laboratory in order to develop a simplified blade-loading parameter based on boundary-layer theory and independent of lift-coefficient terms. A simplified parameter, called the diffusion factor for design angle of attack, was obtained by deriving an approximate relation between a separation criterion used in two-dimensional incompressible turbulent boundary-layer theory (as in ref. 2) and the external velocity diagram and solidity of the blade element. The approximation was facilitated by the use of a model blade-surface velocity distribution and of the local pressure characteristics of blades in two-dimensional cascade at design angle of attack.

An experimental correlation between total-pressure loss coefficient at design angle of attack and a large number of proposed separation parameters is presented for the two-dimensional cascade data of reference 3. In addition, a further correlation between the loss coefficient and the derived diffusion factor is presented for the hub-, tip-, and mean-radius regions of rotors and stators of a large number of experimental single-stage axial-flow compressors.

SYMBOLS

The following symbols are used in this report:

a	ratio of distance from leading edge to point of maximum suction-surface velocity to chord length
b	constant in diffusion-factor equation
C_D	drag coefficient
C_L	lift coefficient
C_s	stalling coefficient of reference 1
c	chord length
D	diffusion factor
d	constant in diffusion-factor equation
F	force
F_D	drag force
H	boundary-layer form factor (ratio of displacement thickness to momentum thickness)
i	angle of incidence, angle between inlet-air direction and blade mean-line direction at leading edge
L	lift force
M	Mach number
n	constant in separation-criterion equation
P	total pressure

[redacted]

p	static pressure
q	constant
R	reaction or recovery ratio
Re	momentum-thickness Reynolds number
r	radius
s	blade spacing
T	total temperature
t	static temperature
V	velocity
$\overline{V}$	circumferentially averaged velocity
V_{av}	average velocity between V_{max} and V_2
V_{max}	maximum velocity on suction surface
x	distance along flow path
α	angle of attack, angle between inlet-air direction and blade chord
β	air angle
Γ	velocity-gradient parameter of reference 2
γ	ratio of specific heats
η	adiabatic temperature-rise efficiency
θ	boundary-layer momentum thickness
ρ	static density
σ	solidity
τ	shear stress
$\overline{\omega}$	relative total-pressure loss coefficient, $P_{2,1} - P_2/P_1 - p_1$

[redacted]

Subscripts:

a	axial
i	ideal
m	vector mean
R	rotor
ref	reference
S	stator
θ	tangential
1	inlet
2	outlet

The prime refers to relative conditions for rotating elements.

ANALYSIS

Approach

Exclusive of three-dimensional effects in the end regions of blade rows, the development of friction boundary layers along the surfaces of compressor blade elements is determined primarily by the surface pressure distributions and therefore by the basic geometry of the element (profile shape, camber, thickness, solidity, and angle of incidence). Therefore, a first approach to the problem of boundary-layer growth and separation can be made by considering the two-dimensional flow about blade elements. Although several techniques are available for computing boundary-layer growth in two-dimensional cascades (refs. 4 to 6), they depend on a prior knowledge of the pressure or velocity distribution about the blade section. However, accurate practical methods of computing compressible pressure distributions about arbitrary compressor cascade sections are not as yet available.

In view of the general complexity and incompleteness of current boundary-layer and pressure-distribution theory, the accurate calculation of the boundary-layer development and total-pressure loss of a given blade element was not believed to be currently feasible. It was decided, therefore, as a first approach, to investigate the possibility of deriving a simplified and approximate blade-loading or separation criterion. The approximate separation criterion might then, in conjunction with an extensive experimental correlation, provide a simple and useful means of determining regions of safe or unsafe limiting design conditions for the actual compressor.

[redacted]

For conventional compressors, in general, differences in blade shape, boundary-layer Reynolds number, turbulence level, transition from laminar to turbulent flow, and Mach number are not very great; so that, comparatively, the most significant factors influencing the pressure distribution and the loss of a blade element are the angle of incidence and the circulation about the element. Furthermore, if attention is restricted to the design point (design angle of incidence), it would be expected that the basic velocity vector diagram of the element at design would be the largest factor affecting the loss. The problem is then reduced to deriving a satisfactory, simplified, and approximate relation between the limiting diffusion gradient on the blade suction surface and the over-all velocity change across the blade row as determined by the design velocity diagram.

Diffusion Factor

A parameter frequently used in establishing a separation criterion in incompressible, two-dimensional, turbulent boundary-layer theory (refs. 2 and 7, for example) is given by

$$D = -\frac{\theta}{V}\frac{dV}{dx}\,Re^{n} \tag{1}$$

where θ is the boundary-layer momentum thickness, V is the free-stream velocity outside the boundary layer, x is distance along the direction of flow, Re is the momentum-thickness Reynolds number, and n is a constant (negative value). The significance of equation (1) can be seen from inspection of the general momentum boundary-layer equation

$$\frac{d\theta}{dx} = \frac{\tau}{\rho V^{2}} - (H + 2)\,\frac{\theta}{V}\frac{dV}{dx} \tag{2}$$

where τ is the viscous shear stress at the surface, H is boundary-layer form factor (ratio of displacement thickness to momentum thickness), and ρ is free-stream density. For configurations with fairly large adverse velocity gradients - as in the case for compressor blade suction surfaces - rapid rates of boundary-layer growth are associated primarily with the last term of equation (2) involving the velocity gradient dV/dx. In fact, for incipient separation, the shear stress τ approaches zero, and the form factor H approaches an approximately constant value of about 2.0 to 2.5 (refs. 6 and 7). Equation (2) therefore becomes

$$\frac{d\theta}{dx} \cong \text{constant}\left(-\frac{\theta}{V}\frac{dV}{dx}\right) \tag{3}$$

Equation (3) shows that the first factor on the right side of equation (1) is proportional to the gradient, or growth rate, of the momentum thickness θ at the point of incipient separation.

In order to evaluate the importance of the second factor, Re^n, in equation (1), it is assumed that, for typical velocity distributions, the local value of Re is related to the initial value of Re at the start of deceleration. Inasmuch as the flow on the suction surface was previously accelerating, the initial value of Re defines the condition of the initial boundary layer (ref. 6). Thus the Re^n term in equation (1) reflects the additional effect of the state of the initial boundary layer. In general, the greater the magnitude of Re, the smaller the allowable diffusion at separation (refs. 6 and 8).

For conventional compressors - and certainly for a given cascade investigation - the range of variation of initial boundary-layer Reynolds number, as influenced by such factors as blade size, inlet Mach number, surface roughness, and turbulence level, is generally not large.

The effect of initial boundary-layer Reynolds number can thus be represented by a constant average value. A simplified separation criterion is therefore adopted as the diffusion factor:

$$D = -\frac{\theta}{V}\frac{dV}{dx} \tag{4}$$

The variation of velocity over the surfaces of a typical compressor blade section set at its design angle of attack is shown in figure 1, and the element velocity diagram is shown in figure 2. By design angle of attack is meant the angle of attack at minimum loss. Diffusion of the suction-surface velocity must occur from the peak velocity near the leading edge V_{max} to the outlet velocity V_2. (It is assumed that V_2 at the blade trailing edge is equal to the mean V_2 considered by the velocity diagram at the downstream measuring station of the blade row.) For most conventional blade designs, the velocity generally varies approximately linearly from V_{max} to V_2. The diffusion gradient can then be approximated on the average by

$$-\frac{1}{V}\frac{dV}{dx} \approx -\frac{V_{max} - V_2}{(1-a)cV_{av}} \tag{5}$$

where V_{av} is some average surface velocity between V_{max} and V_2. The use of equation (5) is expected to be valid for moderately nonlinear velocity variations as well, since recent unpublished results of boundary-layer analyses conducted at the NACA Langley laboratory indicate that the over-all diffusion $V_{max} - V_2$ is the significant factor affecting limiting loading.

[redacted]

From examination of velocity distributions about typical compressor blade sections, it was found that the average velocity V_{av} in the denominator of equation (5) can be approximated by V_1, so that equation (5) can be given by

$$-\frac{1}{V}\frac{dV}{dx} = \frac{1}{(1-a)c}\left[\left(1 - \frac{V_2}{V_1}\right) + \left(\frac{V_{max}}{V_1} - 1\right)\right] \tag{6}$$

In general, the magnitude of the maximum suction-surface velocity can be considered to be composed of several components so that, as shown in figure 1,

$$V_{max} = \overline{V} + \Delta V = V_1 + \Delta\overline{V} + \Delta V \tag{7}$$

where $\Delta\overline{V}$ represents the velocity increment due to chordwise variations of the circumferentially averaged velocity (function of ratio of blade thickness to blade spacing and of inlet Mach number), and ΔV represents the velocity increment above the value of $\overline{V}$ that arises from the blade loading or circulation (function of profile shape and angle of attack). In terms of inlet velocity, equation (7) can be expressed as

$$\frac{V_{max}}{V_1} - 1 = \frac{\Delta V}{V_1} + \frac{\Delta\overline{V}}{V_1} \tag{8}$$

In hypothesizing a functional relation between maximum velocity ratio and circulation as indicated in equation (8), use was made of the characteristics of blade sections in low-speed, two-dimensional cascade. The similarity of surface pressure distributions for a given blade section in cascade and in the compressor configuration in the region of design angle of attack is demonstrated in reference 9. From examination of the pressure distributions about the NACA 65-series blade sections in cascade (ref. 3), it was deduced that a functional relation can be established between the velocity ratio and a circulation parameter $\Delta V_\theta/\sigma V_1$ (proportional to lift coefficient) in the form

$$\frac{V_{max}}{V_1} - 1 = b\frac{\Delta V_\theta}{\sigma V_1} + d \tag{9}$$

where d represents the surface-velocity rise due to the effect of finite blade thickness indicated in equation (8). In general, both b and d may vary with blade shape, angle of incidence, and inlet Mach number. If it is then assumed that equation (9) is valid for conventional compressor blades, the diffusion parameter D can be expressed as

$$D = \frac{\theta}{(1-a)c}\left[\left(1 - \frac{V_2}{V_1}\right) + b\frac{\Delta V_\theta}{\sigma V_1} + d\right] \tag{10}$$

If it can further be assumed, for simplicity, that the average ratio of boundary-layer momentum thickness to chord length, θ/c, and the location ratio, a, vary very little for conventional types of blading, then, on the average

$$\frac{\theta}{(1-a)c} = \text{constant}$$

and the diffusion parameter can then be reduced to the form

$$D = \left(1 - \frac{V_2}{V_1}\right) + b\,\frac{\Delta V_\theta}{\sigma V_1} + d \tag{11}$$

Average values of b and d obtained from examination of the data of reference 3 at design angle of attack were about 0.4 to 0.5 and about 0.1, respectively. The design angle of attack for the cascade data was taken as the value of incidence at the midpoint of the low-loss range. In checking the trend of the effect of compressibility on the value of b and d obtained from the low-speed data, it was found that, if the local pressure coefficient and the circulation parameter both varied in the same manner with Mach number (say, the Prandtl-Glauert relation), the increases in magnitude of b and d at the design angle of attack up to Mach numbers of about 0.75 would be small. Values of b and d were consequently taken as 0.5 and 0.1, respectively, to give

$$D = \left(1 - \frac{V_2}{V_1}\right) + \frac{\Delta V_\theta}{2\sigma V_1} + 0.1 \tag{12}$$

Since there are generally small differences in thickness and thickness distribution for commonly used blades, the last term in equation (12) will not vary much, and the design diffusion factor D for a compressor blade element is finally established as

$$D = \left(1 - \frac{V_2}{V_1}\right) + \frac{\Delta V_\theta}{2\sigma V_1} \tag{13}$$

where all velocities are taken relative to the blade.

The suction-surface diffusion is thus seen to be a function of two principal factors: the over-all change in relative velocity across the element, and a term proportional to the conventional lift coefficient of the section based on inlet velocity

$$C_{L,1} = \frac{2\Delta V_\theta}{\sigma V_1} \frac{\cos \beta_1}{\cos \beta_m}$$

For two-dimensional flow with equal axial velocities at inlet and outlet, the diffusion factor of equation (13) becomes (see fig. 2)

$$D = \left(1 - \frac{\cos \beta_1}{\cos \beta_2}\right) + \frac{\cos \beta_1}{2\sigma} (\tan \beta_1 - \tan \beta_2) \qquad (14)$$

The general similarity between the derived design diffusion factor of equation (13) and the stalling coefficient of reference 1 is illustrated by the expansion of equation (A8) in appendix A with $V_m \cong \frac{1}{2}(V_1 + V_2)$ to give

$$C_s = \frac{2}{1 + \frac{V_2}{V_1}} \left[\frac{2}{q}\left(1 - \frac{V_2}{V_1}\right) + \frac{2\Delta V_\theta}{\sigma V_1}\right] \qquad (15)$$

where q is a constant varying between 1 and 2. The velocity gradient parameter Γ of reference 2, in contrast, involves a product of the lift coefficient and the over-all velocity-ratio terms (eq. (A9), appendix A).

RESULTS AND DISCUSSION

Two-Dimensional Cascade

The general validity of the various blade-loading parameters and separation criteria commonly used in axial-flow-compressor design was first investigated for the extensive low-speed cascade data for the NACA 65-series compressor blade sections as given in reference 3. The analysis was made by examining the variation of blade-element total-pressure loss with various loading parameters at design angle of attack. The total-pressure loss was expressed in terms of a loss coefficient $\bar{\omega}$, as defined in appendix B. For the cascade data, the total-pressure loss coefficient was computed from the drag coefficients (based on inlet conditions) given in reference 3 according to equation (B17) in appendix B. Design angle of attack for the loss evaluation was taken as the midpoint of the minimum drag range. Loading parameters considered were: (1) theoretical lift coefficient based on vector-mean velocity, (2) solidity multiplied by theoretical lift coefficient based on vector-mean velocity, (3) theoretical lift coefficient based on inlet velocity, (4) theoretical lift coefficient based on outlet velocity, (5) over-all reaction or recovery ratio, (6) relative velocity ratio, (7) velocity-gradient

parameter of reference 2, (8) stalling coefficient of reference 1, and (9) diffusion factor given by equation (14). The various theoretical lift-coefficient equations and loading parameters are given in appendix A. The resulting comparison of total-pressure loss coefficient against loading parameter is shown in figure 3. Each curve in figure 3 represents the variation of loss coefficient for the range of cambers used at each fixed condition of solidity and inlet-air angle.

From figure 3 it is seen, as expected, that the loss tends to increase gradually with increasing blade loading, and that, particularly at inlet angles of 60° and 70°, a sharp rise in loss indicative of separation occurs beyond a certain value of the blade loading. For the various blade-loading parameters plotted in figure 3, it is seen that only the outlet lift coefficient (fig. 3(d)), Howell's gradient parameter (fig. 3(g)), Wislicenus' stalling parameter (fig. 3(h)), and the diffusion factor D (fig. 3(i)) can be considered as acceptable limiting criteria.

For Howell's parameter (fig. 3(g)), a limiting value of about 4.5 to 5.0 is indicated; and for the stalling coefficient of Wislicenus (fig. 3(h)), the limiting value is about 2.0 for $q = 1.0$. For the diffusion factor (fig. 3(i)), the point of loss rise occurs at a value of D of about 0.6. It is interesting to note that one of the more common limiting-loading parameters of $\sigma C_{L,m} = 1.0$ to 1.2 (ref. 10, e.g.) corresponds to the point of loss rise for an inlet angle of about 60° and solidity from 0.5 to 1.0 (fig. 3(b)), conditions which are closely descriptive of rotor-tip velocity diagrams. This same limit, however, (as was indicated in ref. 3) would not be valid for other conditions of solidity and inlet angle for these data.

With the establishment of the diffusion factor as a satisfactory loading limitation for design blade-element loss, it is interesting to examine briefly some of the other coexisting factors, such as solidity, inlet Mach number, and Reynolds number, which influence the magnitude of the loss. A cross plot of the data of figure 3(i) for subcritical (below limiting value) diffusion factors indicates that the loss coefficient varies primarily with solidity and to a smaller extent with inlet angle. The loss variation with solidity for $D = 0.5$ is illustrated in figure 4(a). For the usual range of inlet angles from 40° to 60° it can be taken roughly that the loss coefficient will vary directly with the solidity (as a reflection of the increased friction surface), as long as the critical diffusion rate is not exceeded.

A second significant factor in blade-element performance is the general compressibility effect and the formation of surface shocks and boundary-layer separation. An illustrative variation of total-pressure loss coefficient with inlet Mach number for a 65-series blade element is

shown in figure 4(b). The curve was obtained from the data of reference 11 and recomputed in terms of the loss coefficient used in this report. The value of inlet Mach number at which the losses tend to rise sharply is called the limiting inlet Mach number. In general, the limiting Mach number will vary with diffusion factor, inlet angle, and solidity.

The effect of blade-chord Reynolds number on loss coefficient is shown in figure 4(c) for the data of reference 3. In general, the loss is seen to increase with decreasing Reynolds number, but no sharp rise in loss is observed for the lowest values of Reynolds number obtained in the tests.

Thus for the cascade blade, as long as the limiting diffusion factor and limiting inlet Mach number are not exceeded, design blade-element total-pressure loss coefficient will not be excessive for the usual range of solidity, Reynolds number, and blade shape. The exact selection of the magnitudes of these factors of diffusion, solidity, and Reynolds and Mach numbers, of course, will depend on the particular design application and such considerations as range of operation, off-design characteristics, size, and three-dimensional effects.

Compressor Rotor

In view of the success of the diffusion factor in establishing a consistent loading limitation for the 65-series cascade blade, a further analysis was made to ascertain the general validity of the diffusion limit for blades in the actual compressor configuration. A correlation was obtained between measured relative total-pressure loss coefficient and calculated diffusion factor across blade elements in the hub, tip, and mean regions of a large number of experimental axial-flow single stages over a range of tip speeds. A transonic rotor, as well as conventional subsonic designs, was included in the comparison. Details of the various rotor designs and blade shapes from which the data were obtained are given in table I.

The diffusion factor was computed according to equation (13) from the measured velocities at blade inlet and outlet obtained from radial surveys. The total-pressure loss coefficient relative to the rotor blade element was computed from the measurements of absolute total-pressure ratio and total-temperature ratio and the relative inlet Mach number according to the development in appendix B (eq. (B9)). For the blade rows with varying hub radius, the inlet and outlet flow conditions were taken along approximated streamlines, and the solidity term in equation (13) was taken as an average value. The effect of the ideal relative total-pressure ratio (eq. (B4)) on the computed loss coefficient (eq. (B3)) was negligible for the range of wheel speed and change in

radius of the streamline flow of the stages investigated. Data for the blade-end regions were taken at points from 10 to 12 percent of the passage height from the outer wall for the tip region, and from 10 to 16 percent of the passage height from the inner wall for the hub region, depending on the particular survey program of each compressor. In all cases these tip and hub locations were outside the wall boundary regions. In order to obtain data representing the design angle of attack, plots of blade-element relative loss coefficient (and efficiency) against diffusion factor were made for each tip speed run as illustrated in figure 5, and the point of minimum loss was determined from the faired curves.

Hub- and mean-radius regions. - The variation of minimum relative total-pressure loss coefficient with diffusion factor at the mean- and hub-radius regions of ten single-stage rotor configurations is presented in figure 6 for sub-limiting relative inlet Mach numbers. In the figure are also shown (dotted lines) the expected variation of loss coefficient based on cascade characteristics for average conditions of solidity and inlet angle ($\sigma = 1.2$, $\beta_1' = 50^\circ$ for mean; and $\sigma = 1.5$, $\beta_1' = 40^\circ$ for hub) at inlet Mach numbers of 0.1 and 0.75. The values of loss at the low Mach number were obtained from the data of reference 3, and the values of loss at the high Mach number were obtained from the use of ratios of compressible loss to incompressible loss as determined from figure 4(b). For the hub- and mean-radius regions, no marked variation of loss coefficient with diffusion factor is found, with a large accumulation of points between a loss of zero and about 0.1 up to a diffusion factor of about 0.6.

It is seen that quite a few points are obtained both below and above the anticipated loss levels for blade-element flow as deduced from the cascade data. Aside from possible differences in solidity, blade shape, and Reynolds number, the data points above the upper cascade limit can be attributed to three-dimensional and unsteady-flow effects in the rotating blade row or to experimental error. In view of the many points at zero or close to zero loss, a good deal of the scatter is suspected to be the result of experimental error. Small inaccuracies in measurements and in determining the correct streamline locations at inlet and outlet can result in significant errors in the loss determination. For example, an error of $\pm 1^\circ$ F in outlet temperature at a pressure ratio of 1.20 will result in computed loss values of from 0.011 to 0.050 for a true efficiency of 0.95 and from 0.042 to 0.082 for a true efficiency of 0.90. At an efficiency of 0.90 and a pressure ratio of 1.4, the spread of the loss error is somewhat smaller (0.033).

In view of these considerations, the rotor data of figure 6 for hub and mean regions are interpreted as an adequate confirmation of the loss trend with diffusion factor as established from the cascade data up to

values of at least about 0.55. Unfortunately, values of diffusion factor greater than about 0.55 were not obtained in the tests, so that a comparison of limiting values of diffusion factor could not be made. It appears, however, that no difficulty with limiting loading or separation should be experienced in the hub- and mean-radius regions of the rotor for design diffusion factors up to about at least 0.55, provided the limiting relative inlet Mach number for the particular blade profile is not exceeded.

Further confirmation of an inlet Mach number limitation in the compressor configuration was observed for the NACA 65-series rotor blades of about 10 percent maximum thickness at the mean radius, as shown by the loss-coefficient plots of figure 7. The dashed line indicates the expected loss variation as obtained from cascade tests (ref. 11). A marked rise in loss is observed for relative inlet Mach numbers greater than about 0.7 to 0.75. The diffusion factors of the data points at the high Mach number values were less than 0.6. (These high Mach number points were not included in the plot of fig. 6(a).) A similar compressibility effect for the hub region could not be definitely established because of the generally lower levels of inlet Mach numbers in this region. It can reasonably be assumed, therefore, that, for the conventional NACA 65-series blades of 10 percent thickness ratio, Mach number difficulties will be avoided (for subcritical diffusion factors) at hub- and mean-radius regions of the rotor if the relative inlet Mach number does not exceed a value of about 0.7 to 0.75. For other types of blade and thickness variations, of course, the limiting Mach number range will be different.

Tip region. - The variation of minimum (design) relative total-pressure loss coefficient with diffusion factor in the tip region of the rotor is shown in figure 8. As before, the dashed lines represent the range of loss indicated by the cascade data ($\sigma = 0.9$, $\beta_1' = 60^\circ$). In marked contrast to the hub- and mean-radius correlations, the tip-region plot shows a greater range of loss values and diffusion factor with a very definite and essentially linear increase in loss coefficient with diffusion factor. The trend of the loss variation below values of D of 0.3 could not be established because of insufficient data. It is expected that the loss coefficient will remain approximately constant as the diffusion factor approaches zero. The corresponding variation of maximum blade-element temperature-rise efficiency with diffusion factor is shown in figure 9. For a tip-region efficiency of 0.90, diffusion factors no greater than approximately 0.45 are indicated.

The early deterioration of the flow in the rotor tip region is believed to be the result of tip losses and three-dimensional effects such as clearance leakage, casing boundary-layer growth and scrubbing, secondary flows, and radial displacement of low-energy fluid out toward the rotor tip. Exactly which factors or combination of factors contributes most to the premature rise in loss is not presently known and

should constitute an important aspect of future research. In view of the fact that the flow in the tip region is not a "blade-element" or profile flow, the strength of the tip-region correlation with diffusion factor suggests that the local (or over-all) static-pressure gradients that exist in the blade-end regions (imposed by the blade element) play an important role in the complex tip-loss phenomena.

It was also observed that a correlation between loss coefficient and diffusion factor can be obtained for all loss values in the positive range of angle of incidence (increasing diffusion factor) from the region of minimum loss coefficient to values corresponding to a decrease in efficiency of about 0.10 to 0.15 (see fig. 5(a)). The resulting plot is shown in figure 10. The correlation of figure 10 results from the fact that the average slope of the variation of loss against diffusion factor in the positive incidence range (see fig. 5) is roughly equal to the slope of the original plot of minimum loss coefficient (design incidence angle) against diffusion factor shown in figure 8. The data of figure 10 may find use in estimating tip-region losses at positive incidence (low weight flow) off-design conditions.

In figure 8, for the rotors with 65-series blade shapes, only the two highest loss points of rotor 1 were at relative inlet Mach numbers substantially greater than the limiting values indicated in figure 7. The effect of inlet Mach numbers above the limiting values is markedly shown in the efficiency plot of figure 9 and in the loss plot of figure 8. Theoretically, the general plots of loss coefficient against diffusion factor as derived herein would be expected to be a family of curves with relative inlet Mach number as parameter. Within the limits of experimental accuracy, a correlation of experimental loss data in terms of diffusion factor may provide a means for separating the individual loss contributions arising from blade loading (conventional surface-velocity gradients) and shock effects (boundary-layer interaction and wave formation).

The scatter of the data in figures 8 and 9 is attributed primarily to differences in tip losses, in the locations of the tip-region survey stations (efficiency gradients are large in this region), and to experimental inaccuracies. For example, for a pressure ratio of 1.2 at a true efficiency of 0.85, an error in outlet temperature of $\pm 1^{\circ}$ F results in total-pressure loss values of 0.079 to 0.138. As an alternate method which circumvents the direct use of temperature-rise efficiency, the relative total-pressure loss can be determined from the computed relative total-pressure ratio as indicated by equations (B2) and (B6). However, experimental inaccuracies are likely to be encountered in this procedure, also.

It was impossible to evaluate the relative significance of the two contributing terms (the velocity ratio and the circulation parameter)

in the diffusion factor, as there was no consistent variation between the terms or dominance of one term over the other. At least for the cascade (as indicated by figs. 3(f) and (i)), both terms appear to be about equally significant. The value of 0.5 taken for the constant b in the circulation term of equation (11) appears to be quite satisfactory in view of the resulting correlation.

Compressor Stator

Loss and diffusion characteristics at design angle of attack for compressor stator blades were also investigated by examining the data from six inlet-stage stator rows, four with NACA 65-series profiles and two with double circular-arc profiles. Details of the blade designs are given in table II. Stator total-pressure loss coefficient was determined from area averages of the circumferential variation of total pressure across a blade spacing as obtained from total-pressure rakes located a short distance downstream of the stator trailing edge. The loss presented is the total-pressure defect due to the blade wake and does not include any possible drop in free-stream total pressure across the stator row. This total-pressure drop was difficult to establish with any degree of acceptable accuracy. Data for the tip region were obtained from locations at 9 to 15 percent of the passage height from the outer wall and at 13 to 16 percent away from the inner wall for the hub. Velocities were obtained from inlet and outlet surveys of pressure and angle. In most cases, only a single midspacing survey was made behind the stators. Plots of total-pressure loss coefficient and diffusion factor against angle of attack (or incidence) were made as illustrated in figure 11, and values of $\bar{\omega}$ and D were taken at the point of minimum loss (design angle of attack).

The variation of minimum loss coefficient with diffusion factor for compressor stators over a range of inlet Mach numbers (rotor tip speeds) is shown in figure 12 for hub, mean, and tip regions. Minimum loss values were not attained in the hub and mean regions at some tip speeds for stator 4, because the data were insufficient to define the loss variation over a wide enough range of incidence angle. All points shown are at values of inlet Mach number below the limiting value. The dashed lines, as before, represent the estimated limits based on cascade performance. (There is very little difference between the minimum blade-element loss for 65-series and circular-arc blade profiles.) In all three regions, no trend of variation of loss coefficient with diffusion factor is observed, with all points falling between 0.01 and 0.05 up to the highest diffusion factors obtained (about 0.6).

A cross plot of minimum loss coefficient against inlet Mach number for all three positions is shown in figure 13 for the stators with NACA 65-series profiles of 10 percent maximum thickness ratio. As in the case

of the rotor mean-radius region (fig. 7), a rise in loss for inlet Mach numbers greater than about 0.70 is indicated. The high Mach number points in figure 13 were at values of diffusion factor less than 0.65. On the basis of the limited information available, it is expected that very low stator losses will occur at design angle of attack, if the design diffusion factors do not exceed about 0.6 and if the limiting inlet Mach number for the particular blade profile is not exceeded (about 0.70 to 0.75 for the 65-series blade of about 10 percent maximum thickness ratio).

Inasmuch as the data for the preceding analyses have been obtained from a two-dimensional cascade and compressor single stages, the derived limiting values and variations will be most valid in the design of the inlet or early stages of a multistage compressor. It is not known to what extent these values can be applied to the later stages where hub-tip ratios are large and where three-dimensional effects become more pronounced. It is also to be noted that the correlations were based on actual measured values rather than on original design values of inlet and outlet velocity. However, if the general design control and methods of flow prediction are good, the derived limiting values can be directly applied as design limits. In this respect, the inlet stages again are in a favorable position, inasmuch as design control is usually best for the early stages.

SUMMARY OF RESULTS

A simplified limiting-blade-loading criterion called the diffusion factor for axial-flow-compressor blade elements was derived from the application of a separation criterion used in two-dimensional boundary-layer theory to the blade suction-surface velocity distribution of a compressor blade element at design angle of attack:

1. From a correlation between minimum blade-element total-pressure loss coefficient and a large number of blade-loading criteria commonly used or proposed for compressor design, it was found that, on the basis of the data for the NACA 65-series compressor blade sections in low-speed, two-dimensional cascade:

a. The derived diffusion factor provided a satisfactory limiting-loading parameter for the NACA 65-series compressor blade sections, in that the limiting value was clearly defined and was independent of solidity or inlet-air angle. At given solidity and inlet-air angle, the total-pressure loss coefficient at design angle of attack increased slightly with increasing diffusion factor up to a value of diffusion factor of about 0.6, after which a rapid rise in loss was observed.

b. The stalling coefficient of Wislicenus and the velocity-gradient parameter of Howell were also adequate limiting-loading parameters.

2. From a correlation between minimum blade-element relative total-pressure loss coefficient and derived diffusion factor for data from several experimental single-stage axial-flow compressors at sub-limiting inlet Mach numbers, it was found that:

a. For the hub- and mean-radius regions of ten rotor blade rows, the plot of minimum relative loss coefficient against diffusion factor showed essentially no significant variation of loss coefficient with diffusion factor up to values of diffusion factor of about 0.55, which was the extent of the available data.

b. In contrast to the rotor hub and mean regions, the loss correlation for the tip region of the rotors revealed a very marked and practically linear variation of loss coefficient with diffusion factor for values of diffusion factor greater than about 0.30. For a tip-region efficiency of 0.90, diffusion factors no greater than approximately 0.45 were indicated.

c. For the hub-, tip-, and mean-radius regions of six stator blade rows, the plot of minimum total-pressure loss coefficient against diffusion factor revealed no variation of loss coefficient with diffusion factor up to values of about 0.60, which was the extent of the available stator data.

d. Further verification of a limiting relative inlet Mach number of about 0.70 to 0.75 at subcritical values of diffusion factor for NACA 65-series profile shapes of about 10 percent maximum thickness ratio was indicated.

Lewis Flight Propulsion Laboratory
National Advisory Committee for Aeronautics
Cleveland, Ohio

[redacted]

APPENDIX A

LOADING PARAMETERS FOR TWO-DIMENSIONAL INCOMPRESSIBLE FLOW

Lift coefficient. - The lift coefficient is defined as the ratio of lift force per unit area to reference dynamic head, $C_L = \frac{L}{\frac{1}{2}c(\rho V^2)_{ref}}$.

From figure 2, the lift is given by

$$L = \frac{F_\theta}{\cos \beta_m} - F_D \tan \beta_m = \frac{\rho s V_a (\Delta V_\theta)}{\cos \beta_m} - F_D \tan \beta_m$$

and

$$C_L = \frac{2s\rho V_a (\Delta V_\theta)}{c \cos \beta_m (\rho V^2)_{ref}} - C_D \tan \beta_m = \frac{2V_a (\Delta V_\theta)}{\sigma \cos \beta_m (V^2)_{ref}} - C_D \tan \beta_m \tag{A1}$$

or, from figure 2, with $V_{a,1} = V_{a,2}$,

$$C_L = \frac{2V_a^2 (\tan \beta_1 - \tan \beta_2)}{\sigma \cos \beta_m (V^2)_{ref}} - C_D \tan \beta_m \tag{A2}$$

For the purpose of establishing design criteria, the drag term is neglected. The theoretical lift coefficients are then obtained as:
Vector mean velocity:

$$C_{L,m} = \frac{2 \cos \beta_m}{\sigma} (\tan \beta_1 - \tan \beta_2) \tag{A3}$$

Inlet velocity:

$$C_{L,1} = \frac{2 \cos^2 \beta_1}{\sigma \cos \beta_m} (\tan \beta_1 - \tan \beta_2) \tag{A4}$$

Outlet velocity:

$$C_{L,2} = \frac{2 \cos^2 \beta_2}{\sigma \cos \beta_m} (\tan \beta_1 - \tan \beta_2) \tag{A5}$$

where

$$\beta_m = \tan^{-1}\left(\frac{V_{\theta,1} + V_{\theta,2}}{2V_a}\right) = \tan^{-1}\frac{1}{2}(\tan\beta_1 + \tan\beta_2)$$

Over-all reaction or recovery ratio. - The over-all reaction or recovery ratio is defined as ratio of static-pressure rise across the blade element to inlet dynamic head, or

$$R = \frac{p_2 - p_1}{P_1 - p_1} = \frac{(P_2 - \frac{1}{2}\rho V_2^2) - (P_1 - \frac{1}{2}\rho V_1^2)}{\frac{1}{2}\rho V_1^2} \tag{A6}$$

Neglecting losses, for the two-dimensional cascade, yields

$$R = 1 - (V_2/V_1)^2 = 1 - (\cos\beta_1/\cos\beta_2)^2 \tag{A7}$$

Stalling coefficient of reference 1. - The stalling coefficient of reference 1 is defined as

$$C_s = C_{L,m} + \frac{1}{q}\left(\frac{V_1^2 - V_2^2}{V_m^2}\right) \tag{A8}$$

where q is a constant between 1 and 2.

Velocity-gradient parameter of reference 2. - The velocity-gradient parameter of reference 2 is given by

$$\Gamma = C_{L,m}\left(\frac{V_1}{V_2}\right)^3 \tag{A9}$$

APPENDIX B

RELATIVE TOTAL-PRESSURE LOSS COEFFICIENT

Compressor Cascade

In order to investigate and generalize the basic phenomena and variations involved in the blade-element flow, it is necessary to consider the basic loss in total pressure relative to the blade element for rotating as well as stationary blades. The relative total-pressure loss coefficient $\bar{\omega}$ across a blade element is defined as

$$\bar{\omega} = \frac{(P_2')_i - P_2'}{P_1' - p_1} \tag{B1}$$

where P' is relative total pressure, p is static pressure, subscripts 1 and 2 refer to blade inlet and outlet, respectively, and all values represent circumferential mass or area averages. When equation (B1) is divided by P_1', the loss coefficient becomes

$$\bar{\omega} = \frac{\left(\frac{P_2'}{P_1'}\right)_i - \frac{P_2'}{P_1'}}{1 - \frac{p_1}{P_1'}} = \left(\frac{P_2'}{P_1'}\right)_i \left[\frac{1 - \frac{P_2'/P_1'}{(P_2'/P_1')_i}}{1 - \frac{p_1}{P_1'}}\right] \tag{B2}$$

or

$$\bar{\omega} = \left(\frac{P_2'}{P_1'}\right)_i \left\{\frac{1 - \frac{P_2'/P_1'}{(P_2'/P_1')_i}}{1 - \left[\frac{1}{1 + \frac{\gamma-1}{2}(M_1')^2}\right]^{\frac{\gamma}{\gamma-1}}}\right\} \tag{B3}$$

where M_1' is the relative inlet Mach number. The ratio in the numerator of equation (B3) is referred to as the relative total-pressure recovery factor. The ideal relative total-pressure ratio is a function of the element wheel speed and the change in radius across the element, according to the equation

$$\left(\frac{P_2'}{P_1'}\right)_i = \left\{1 + \frac{\gamma-1}{2} M_R^2 \left[1 - \left(\frac{r_1}{r_2}\right)^2\right]\right\}^{\frac{\gamma}{\gamma-1}} \tag{B4}$$

[redacted]

where M_R is the wheel rotational Mach number (outlet wheel tangential velocity divided by inlet stagnation velocity of sound).

For stationary blade rows, the total-pressure loss coefficient is reduced in terms of absolute values to

$$\bar{\omega}_S = \frac{1 - \frac{P_2}{P_1}}{1 - \left[\frac{1}{1 + \frac{\gamma-1}{2}(M_1)^2}\right]^{\frac{\gamma}{\gamma-1}}} \tag{B5}$$

For rotating blade rows, since in most cases only stationary (absolute) instrumentation can be employed downstream of rotor rows, the relative loss must be obtained from absolute measurements. The actual relative total-pressure ratio of equation (B2) can be expressed as

$$\frac{P_2'}{P_1'} = \frac{p_2'\left[1 + \frac{\gamma-1}{2}(M_2')^2\right]^{\frac{\gamma}{\gamma-1}}}{p_1'\left[1 + \frac{\gamma-1}{2}(M_1')^2\right]^{\frac{\gamma}{\gamma-1}}} \tag{B6}$$

and, since $p' = p$, the ratio can further be expressed in terms of absolute total pressure as

$$\frac{P_2'}{P_1'} = \frac{P_2\left[1 + \frac{\gamma-1}{2}(M_1)^2\right]^{\frac{\gamma}{\gamma-1}}\left[1 + \frac{\gamma-1}{2}(M_2')^2\right]^{\frac{\gamma}{\gamma-1}}}{P_1\left[1 + \frac{\gamma-1}{2}(M_2)^2\right]^{\frac{\gamma}{\gamma-1}}\left[1 + \frac{\gamma-1}{2}(M_1')^2\right]^{\frac{\gamma}{\gamma-1}}}$$

which, in terms of temperature ratios, becomes (T is total temperature and t is static temperature),

$$\frac{P_2'}{P_1'} = \frac{P_2}{P_1}\left(\frac{\frac{T_1}{t_1}\frac{T_2'}{t_2'}}{\frac{T_2}{t_2}\frac{T_1'}{t_1'}}\right)^{\frac{\gamma}{\gamma-1}} = \frac{P_2}{P_1}\left(\frac{\frac{t_2}{t_1}\frac{T_2'}{T_1'}}{\frac{T_2}{T_1}\frac{t_2'}{t_1'}}\right)^{\frac{\gamma}{\gamma-1}} \tag{B7}$$

Then, with relative and absolute static temperature identical and with

$$\left(\frac{P_2'}{P_1'}\right)_i = \left(\frac{T_2'}{T_1'}\right)^{\frac{\gamma}{\gamma-1}}$$

the actual relative total-pressure ratio becomes

$$\frac{P_2'}{P_1'} = \left(\frac{P_2'}{P_1'}\right)_i \frac{\frac{P_2}{P_1}}{\left(\frac{T_2}{T_1}\right)^{\frac{\gamma}{\gamma-1}}} \tag{B8}$$

The relative total-pressure loss coefficient for rotating blade row is thus obtained from equations (B1), (B2), and (B8) in terms of measured absolute pressure and temperature and relative inlet Mach number as

$$\bar{\omega}_R = \left(\frac{P_2'}{P_1'}\right)_i \left\{ \frac{1 - \frac{P_2/P_1}{(T_2/T_1)^{\frac{\gamma}{\gamma-1}}}}{1 - \left[\frac{1}{1 + \frac{\gamma-1}{2}(M_1')^2}\right]^{\frac{\gamma}{\gamma-1}}} \right\} \tag{B9}$$

where the ideal relative total-pressure ratio is obtained from equation (B4). The relative loss coefficient can then further be related to the blade-element efficiency through the conventional adiabatic relation

$$\eta = \frac{\left(\frac{P_2}{P_1}\right)^{\frac{\gamma-1}{\gamma}} - 1}{\frac{T_2}{T_1} - 1} \tag{B10}$$

Two-Dimensional Cascade

The relation between blade-element total-pressure loss coefficient $\bar{\omega}$ and drag coefficient C_D can be obtained from examination of the force and velocity diagrams for two-dimensional incompressible (low-speed) flow. From figure 2, the drag force is given by

$$F_D = F_\theta \sin \beta_m - F_a \cos \beta_m \tag{B11}$$

With axial velocity equal at inlet and outlet, F_a results only from the change in static pressure across the blade, which in the presence of losses is given by

$$F_a = s(p_2 - p_1) = s\left[\left(P_2 - \tfrac{1}{2}\rho V_2^2\right) - \left(P_1 - \tfrac{1}{2}\rho V_1^2\right)\right]$$

or

$$F_a = s\left[\tfrac{1}{2}\rho(V_1^2 - V_2^2) - \Delta P\right] \tag{B12}$$

The force in the tangential direction is determined by the momentum change in the tangential direction, or

$$F_\theta = s\rho V_a(V_{\theta,1} - V_{\theta,2}) \tag{B13}$$

Equation (B11) is then obtained from equations (B12) and (B13) as

$$\frac{F_D}{s \cos \beta_m} = \rho V_a(V_{\theta,1} - V_{\theta,2}) \tan \beta_m - \left[\tfrac{1}{2}\rho(V_1^2 - V_2^2) - \Delta P\right] \tag{B14}$$

With

$$\tan \beta_m = \frac{V_{\theta,1} - \frac{1}{2}\Delta V_\theta}{V_a} = \frac{V_{\theta,1} + V_{\theta,2}}{2V_a}$$

and

$$V_1^2 - V_2^2 = V_{\theta,1}^2 - V_{\theta,2}^2$$

substitution of these terms into equation (B14) reduces that equation to

$$\frac{F_D}{s \cos \beta_m} = \Delta P \tag{B15}$$

Dividing equation (B15) by inlet dynamic head ρV_1^2, with $c/s = \sigma$, then yields

$$\frac{\sigma F_D}{\cos \beta_m \ \frac{1}{2}\rho c V_1^2} = \frac{\Delta P}{\frac{1}{2}\rho V_1^2} \tag{B16}$$

By definition,

$$C_{D,1} = \frac{F_D}{\frac{1}{2}\rho c V_1^2} \quad \text{and} \quad \bar{\omega} = \frac{\Delta P}{P_1 - p_1} = \frac{\Delta P}{\frac{1}{2}\rho V_1^2}$$

so that, finally

$$\bar{\omega} = \frac{\sigma C_{D,1}}{\cos \beta_m} \tag{B17}$$

In equation (B17) the drag coefficient is related to the inlet dynamic head. For drag coefficient based on mean velocity,

$$V_1^2 = \frac{V_a^2}{\cos^2 \beta_1} = V_m^2 \frac{\cos^2 \beta_m}{\cos^2 \beta_1}$$

so that, equation (B16) becomes

$$\bar{\omega} = \sigma C_{D,m} \frac{\cos^2 \beta_1}{\cos^3 \beta_m} \tag{B18}$$

REFERENCES

1. Wislicenus, George F.: Fluid Mechanics of Turbomachinery. McGraw-Hill Book Co., Inc., 1947.

2. Howell, A. R.: The Present Basis of Axial Flow Compressor Design. Part I. Cascade Theory and Performance. R. & M. No. 2095, British A.R.C., June 1942.

3. Herrig, L. Joseph, Emery, James C., and Erwin, John R.: Systematic Two-Dimensional Cascade Tests of NACA 65-Series Compressor Blades at Low Speeds. NACA RM L51G31, 1951.

4. McGregor, Charles A.: Two-Dimensional Losses in Turbine Blades. Jour. Aero. Sci., vol. 19, no. 6, June 1952, pp. 404-408.

5. Loitsianskii, L. G.: Resistance of Cascade of Airfoils in Gas Stream at Subsonic Velocities. NACA TM 1303, 1951.

6. Maskell, E. C.: Approximate Calculation of the Turbulent Boundary Layer in Two-Dimensional Incompressible Flow. Rep. No. Aero. 2443, British R.A.E., Nov. 1951.

7. Goldstein, Arthur W., and Mager, Artur: Attainable Circulation of Airfoils in Cascade. NACA Rep. 953, 1950. (Supersedes NACA TN 1941.)

8. Donaldson, Coleman du P., and Lange, Roy H.: Study of the Pressure Rise Across Shock Waves Required to Separate Laminar and Turbulent Boundary Layers. NACA TN 2770, 1952. (Supersedes NACA RM L52C21.)

9. Westphal, Willard R., and Godwin, William R.: Comparison of NACA 65-Series Compressor-Blade Pressure Distributions and Performance in a Rotor and in Cascade. NACA RM L51H20, 1951.

10. Johnsen, Irving A.: Investigation of a 10-Stage Subsonic Axial-Flow Research Compressor. I - Aerodynamic Design. NACA RM E52B18, 1952.

11. Briggs, William B.: Effect of Mach Number on the Flow and Application of Compressibility Corrections in a Two-Dimensional Subsonic-Transonic Compressor Cascade Having Varied Porous-Wall Suction at the Blade Tips. NACA TN 2649, 1952.

12. Moses, J. J., and Serovy, G. K.: Some Effects of Blade Trailing-Edge Thickness on Performance of a Single-Stage Axial-Flow Compressor. NACA RM E51F28, 1951.

13. Standahar, Raymond M., and Serovy, George K.: Some Effects of Changing Solidity by Varying the Number of Blades on Performance of an Axial-Flow Compressor Stage. NACA RM E52A31, 1952.

14. Mahoney, John J., Dugan, Paul D., Budinger, Raymond E., and Goelzer, H. Fred: Investigation of Blade-Row Flow Distributions in Axial-Flow-Compressor Stage Consisting of Guide Vanes and Rotor-Blade Row. NACA RM E50G12, 1950.

15. Lieblein, Seymour, Lewis, George W., Jr., and Sandercock, Donald M.: Experimental Investigation of an Axial-Flow Compressor Inlet Stage Operating at Transonic Relative Inlet Mach Numbers. I - Over-All Performance of Stage with Transonic Rotor and Subsonic Stators up to Rotor Relative Inlet Mach Number of 1.1. NACA RM E52A24, 1952.

16. Jackson, Robert J.: Effects on the Weight-Flow Range and Efficiency of a Typical Axial-Flow Compressor Inlet Stage that Result from the Use of a Decreased Blade Camber or Decreased Guide-Vane Turning. NACA RM E52G02, 1952.

[redacted]

TABLE I. - DETAILS OF SINGLE-STAGE ROTORS

Rotor	Description	Blade shape		Maximum thickness, percent		Chord, in.		Solidity		Outer diameter, in.	Inlet hub-tip ratio	Tip speed, ft/sec	Inlet Mach number	Reference	Chord angle, deg	
		Hub	Tip	Hub	Tip	Hub	Tip	Hub	Tip						Hub	Tip
1	Constant work input; no guide vanes	65-series profile		10	8	1.46	1.82	1.2	1.2	14.0	0.80	450, 736, 874, 915	0.4 - 0.93	12	38.6	48.8
		1.4[a]	0.75[a]													
2	Constant work input; symmetrical velocity diagram at mean radius; guide vanes	65-series profile		6	6	1.35	1.35	1.07	0.68	14.0	0.80	669, 753, 836	0.5 - 0.75	13	21.4	35.4
		2.08	1.31													
3	Constant work input; symmetrical velocity diagram at mean radius; guide vanes	65-series profile		6	6	1.35	1.35	1.15	0.92	14.0	0.80	669, 753, 836	0.5 - 0.75	13	21.4	35.4
		2.08	1.31													
4	Constant work input; symmetrical velocity diagram at mean radius; guide vanes	65-series profile		6	6	1.35	1.35	1.69	1.35	14.0	0.80	669, 753, 836	0.5 - 0.75	13	21.4	35.4
		2.08	1.31													
5	Constant work input; symmetrical velocity diagram at hub; guide vanes	65-series profile		10	10	2.80	2.90	1.13	0.89	30.0	0.80	510, 670, 840	0.35 - 0.70	14	28.8	45.9
		1.2	1.2													
6	Transonic; variable work input; no guide vanes	Approximate circular arc		8	5	3.0	3.25	2.05	1.25	17.36	0.525	600, 800, 900, 1000	0.4 - 1.05	15	25.3	47.0
		40[b]	22[b]													
7	Transonic; variable work input; no guide vanes	Approximate circular arc		8	5	3.0	3.25	1.66	1.01	17.36	0.525	600, 800, 900, 1000	0.4 - 1.05	15	25.3	47.0
		40	22													
8	Constant work input; no guide vanes	65-series profile		10	10	1.31	1.31	1.13	0.565	14.00	0.50	548	0.30 - 0.45	16	21.0	58.0
		1.7	0.885													
9	Constant work input; high-turning guide vanes	65-series profile		10	10	1.31	1.31	1.13	0.565	14.00	0.50	552, 838, 1104, 1214	0.30 - 0.75	16	21.0	58.0
		1.7	0.885													
10	Constant work input; low-turning guide vanes	65-series profile		10	10	1.31	1.31	1.13	0.565	14.00	0.50	552, 828, 1104	0.35 - 0.75	16	21.0	58.0
		1.7	0.885													

[a]Isolated lift coefficient.
[b]Camber angle, deg.

TABLE II. - DETAILS OF SINGLE-STAGE STATORS

Stator	Description	Chord, in.		Solidity		Maximum thickness, percent		Outer diameter, in.	Inlet hub-tip ratio	Outlet hub-tip ratio	Inlet Mach number	Rotor tip speed, ft/sec	Chord angle, deg	
		Tip	Hub	Tip	Hub	Tip	Hub						Hub	Tip
1	Constant-camber circular-arc mean line; biconvex thickness distribution; $\varphi = 20^{\circ}$ [a]	3.23	2.68	1.08	1.45	6	8	17.36	0.60	0.60	0.53 - 0.68	800, 1000	34.0	28.0
2	Constant-camber circular-arc mean line; biconvex thickness distribution; $\varphi = 52^{\circ}$	3.25	3.25	1.07	1.64	7	7	17.36	0.622	0.686	0.41 - 0.66	600, 800, 900, 1000	10.0	10.0
3	Constant-camber NACA 65-series mean line; 65-(12)10	1.31	1.31	0.60	1.09	10	10	14.00	0.536	0.564	0.30 - 0.72	552, 1104, 1215	19.5	49.9
4	Constant-camber NACA 65-series mean line; 65-(18)10	1.31	1.31	0.60	1.09	10	10	14.00	0.536	0.564	0.30 - 0.75	552, 1104, 1180	21.0	53.20
5	Constant-camber NACA 65-series mean line; 65-(12)10	1.31	1.31	0.80	1.10	10	10	14.00	0.53	0.551	0.28 - 0.81	412, 620, 825, 990, 1113	17.5	37.8
6	Constant-camber NACA 65-series mean line; 65-(12)10	1.31	1.31	0.60	1.11	10	10	14.00	0.53	0.551	0.28 - 0.87	369, 553, 738, 848	18.2	32.2

[a] φ, camber angle.

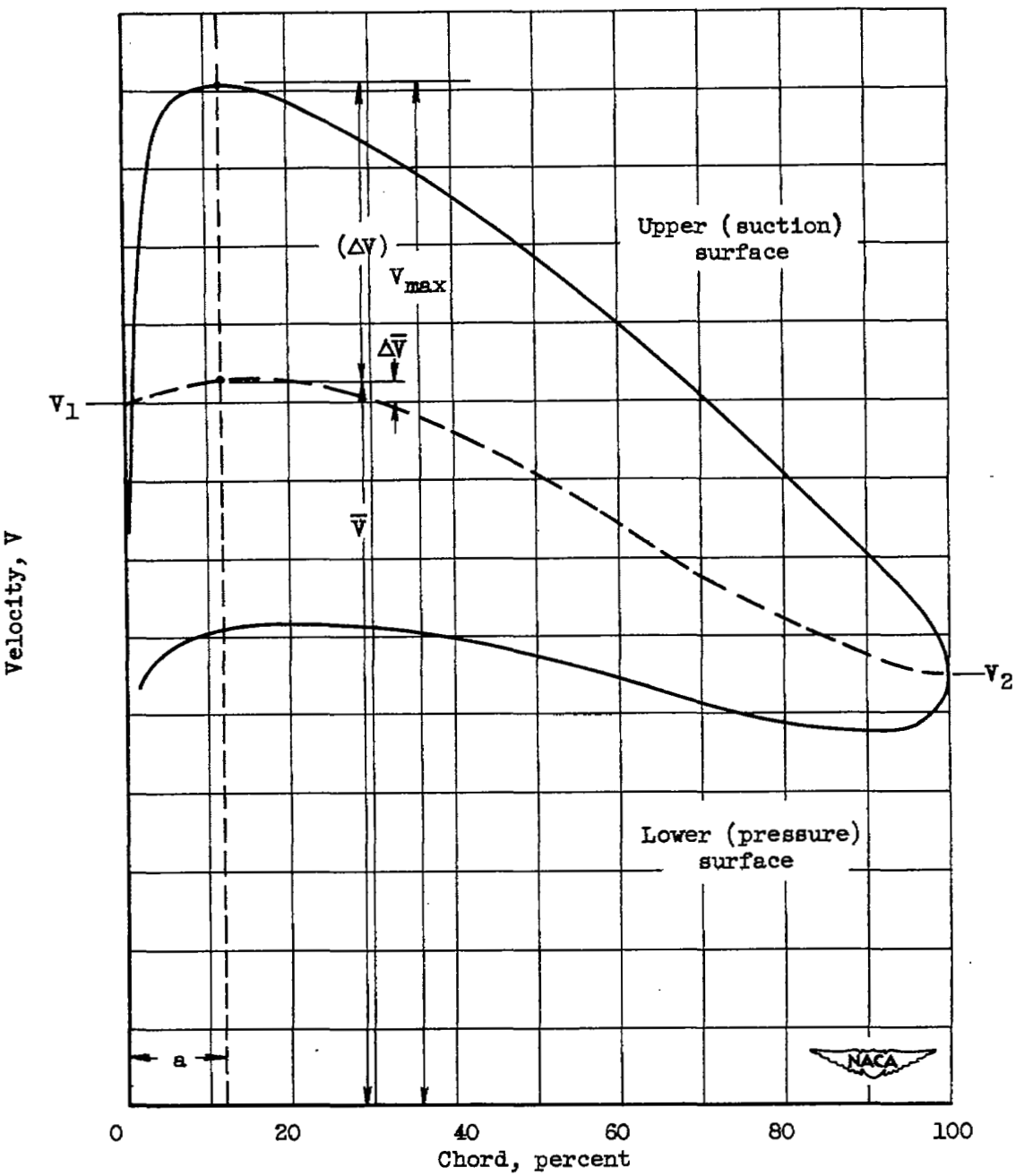

Figure 1. - Typical distribution of velocity along surfaces of compressor-cascade blade section in range of design angle of attack.

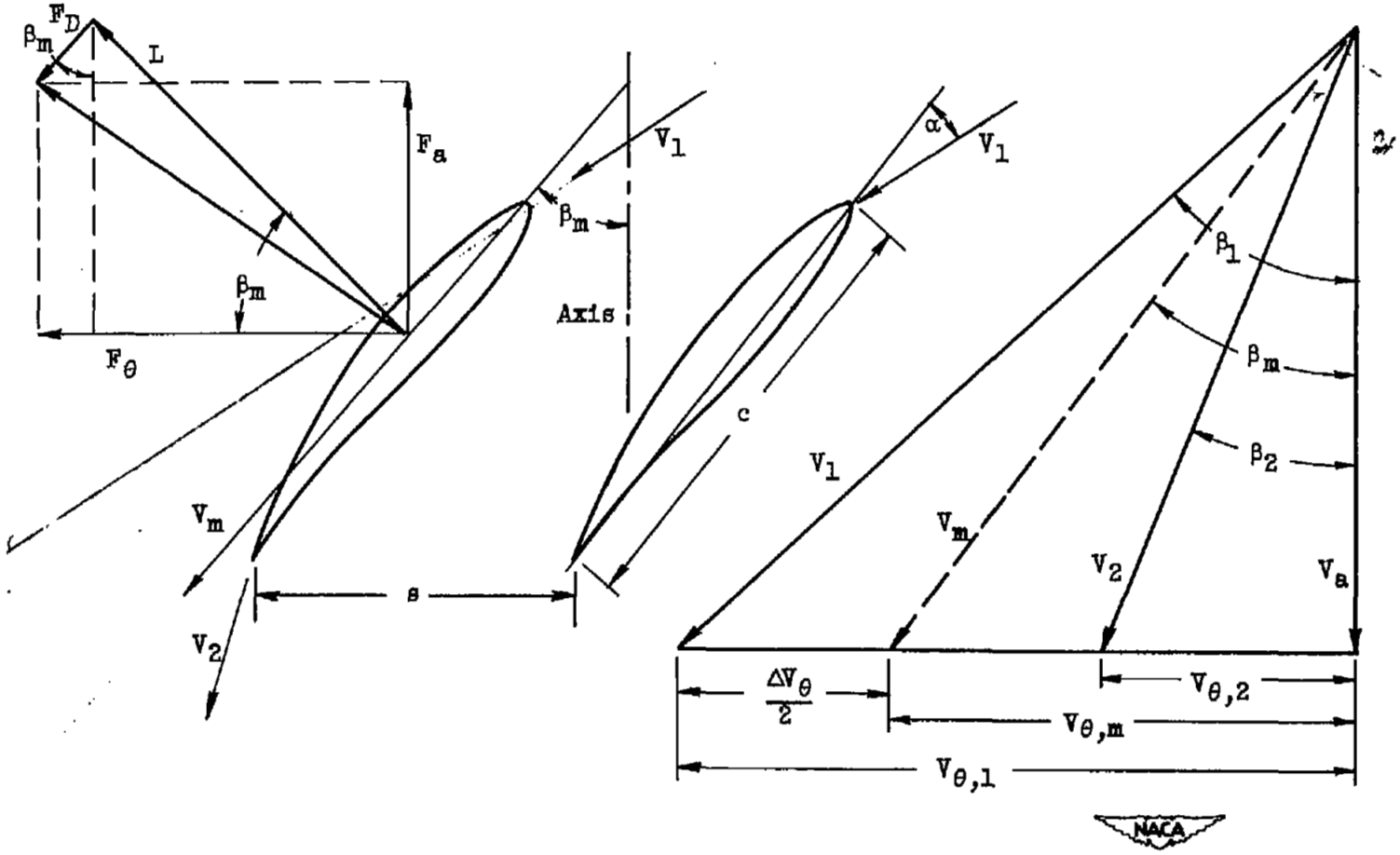

Figure 2. - Force and velocity diagrams for blade in two-dimensional cascade.

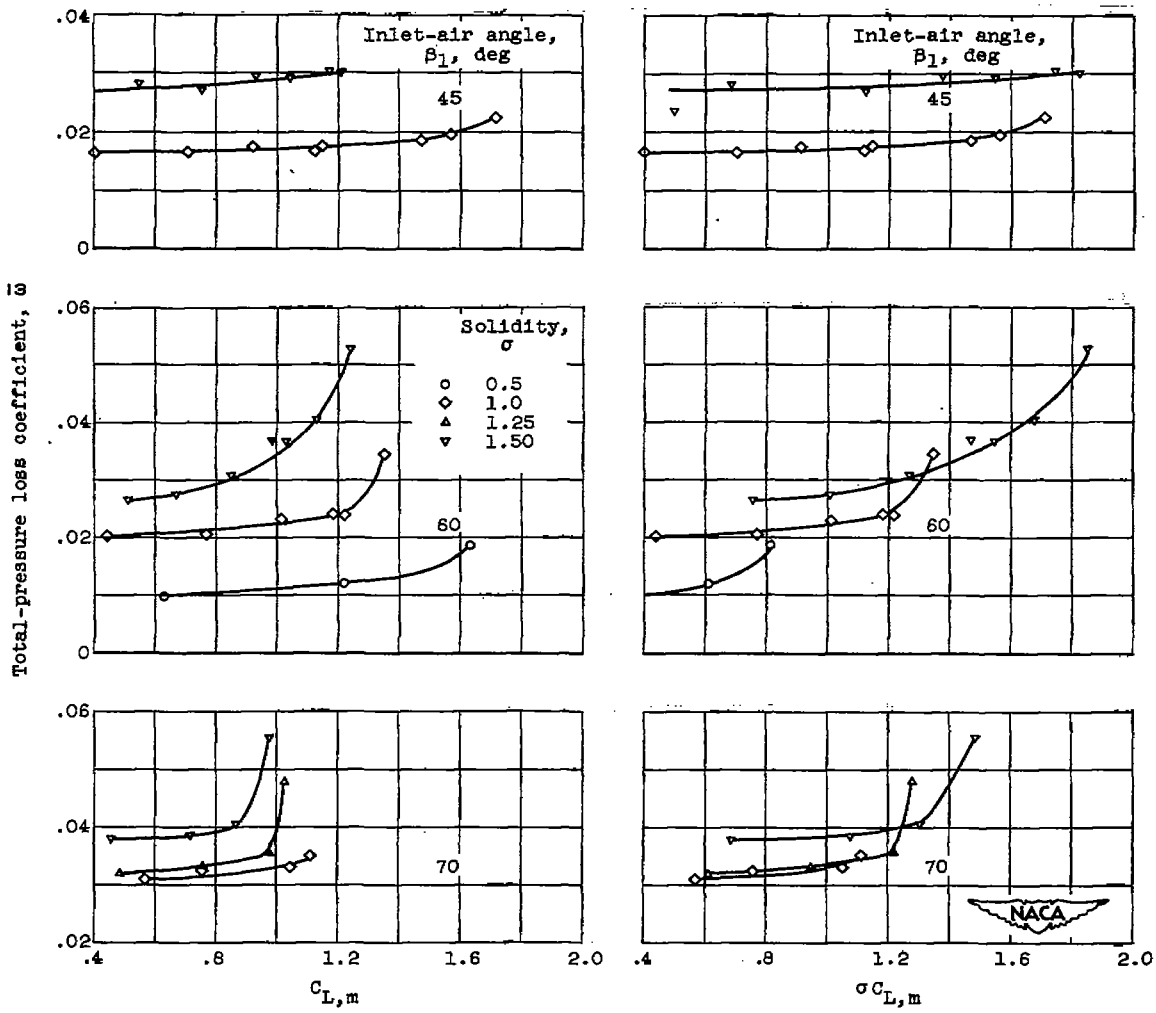

(a) Lift coefficient based on vector-mean velocity.

(b) Solidity times mean-velocity lift coefficient.

Figure 3. - Variation of total-pressure loss coefficient at design angle of attack with various blade-loading parameters for NACA 65-series blade sections in two-dimensional low-speed cascade.

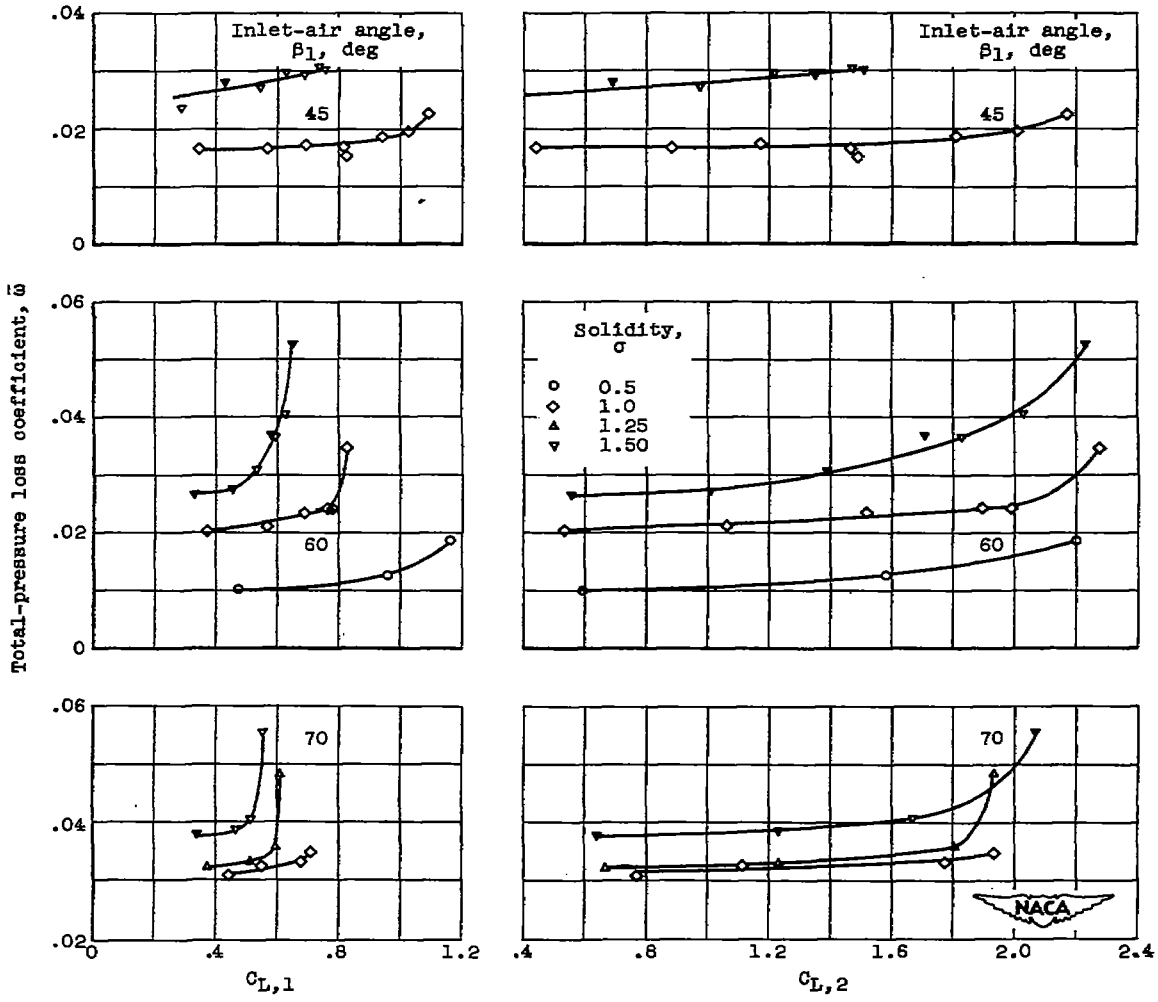

(c) Lift coefficient based on inlet velocity.

(d) Lift coefficient based on outlet velocity.

Figure 3. - Continued. Variation of total-pressure loss coefficient at design angle of attack with various blade-loading parameters for NACA 65-series blade sections in two-dimensional low-speed cascade.

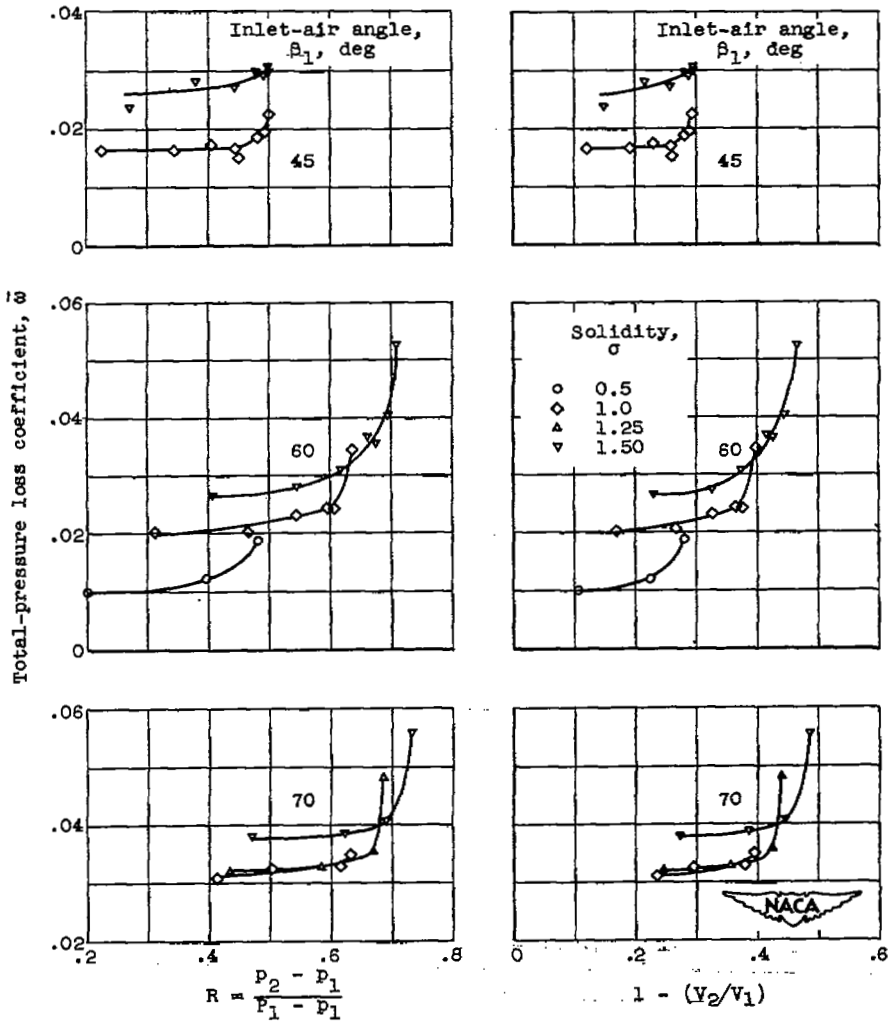

(e) Reaction or recovery ratio. (f) Velocity ratio.

Figure 3. - Continued. Variation of total-pressure loss coefficient at design angle of attack with various blade-loading parameters for NACA 65-series blade sections in two-dimensional low-speed cascade.

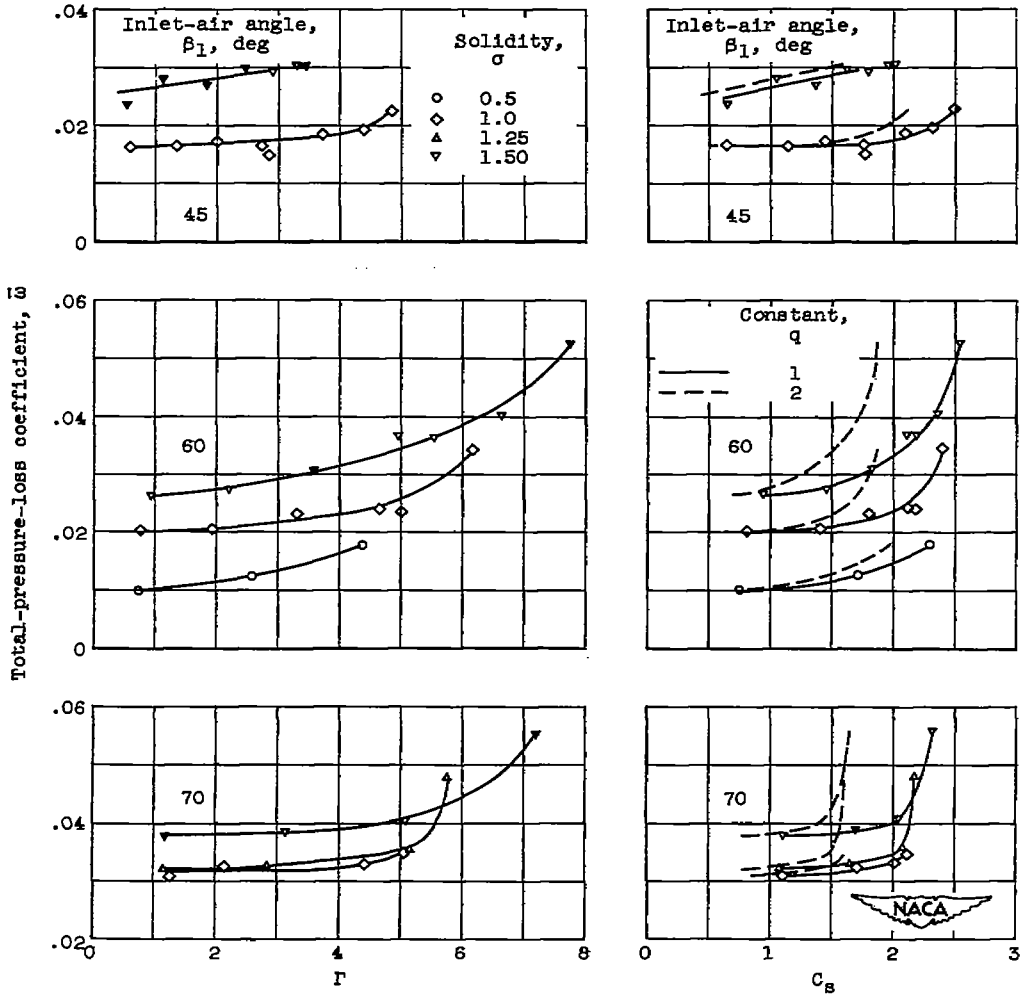

(g) Velocity-gradient parameter of reference 2 (eq. B9).

(h) Stalling coefficient of reference 1 (eq. B8).

Figure 3. - Continued. Variation of total-pressure loss coefficient at design angle of attack with various blade-loading parameters for NACA 65-series blade sections in two-dimensional low-speed cascade.

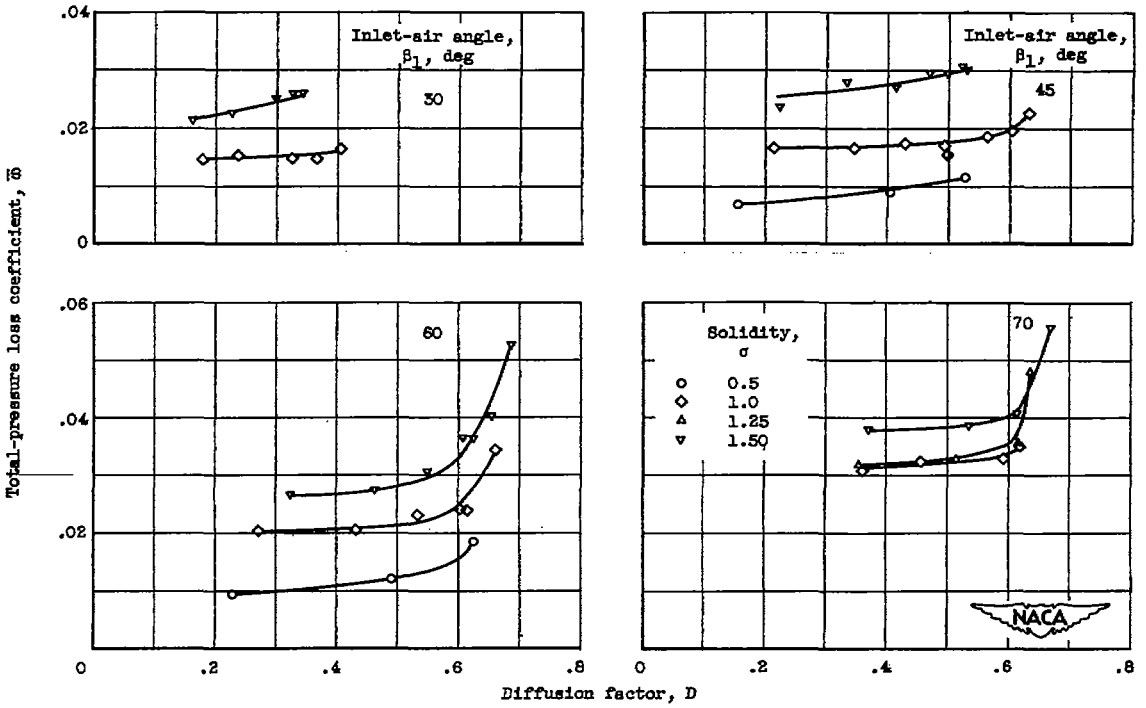

(i) Diffusion factor (eq. (14)).

Figure 3. - Concluded. Variation of total-pressure-loss coefficient at design angle of attack with various blade-loading parameters for NACA 65-series blade sections in two-dimensional low-speed cascade.

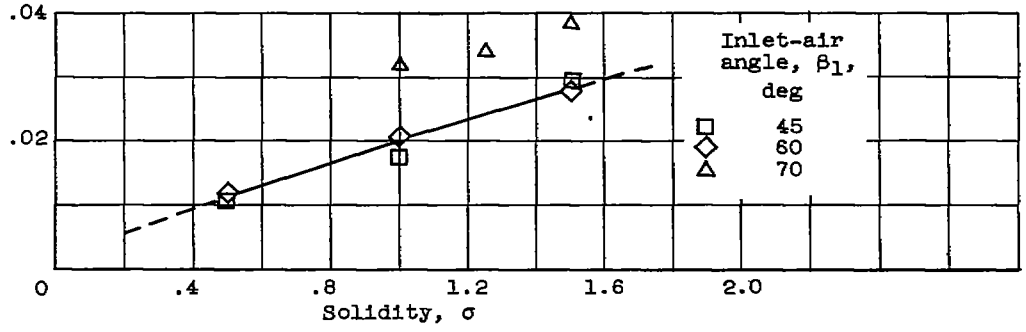

(a) Solidity for diffusion factor of 0.5 (fig. 3(i)).

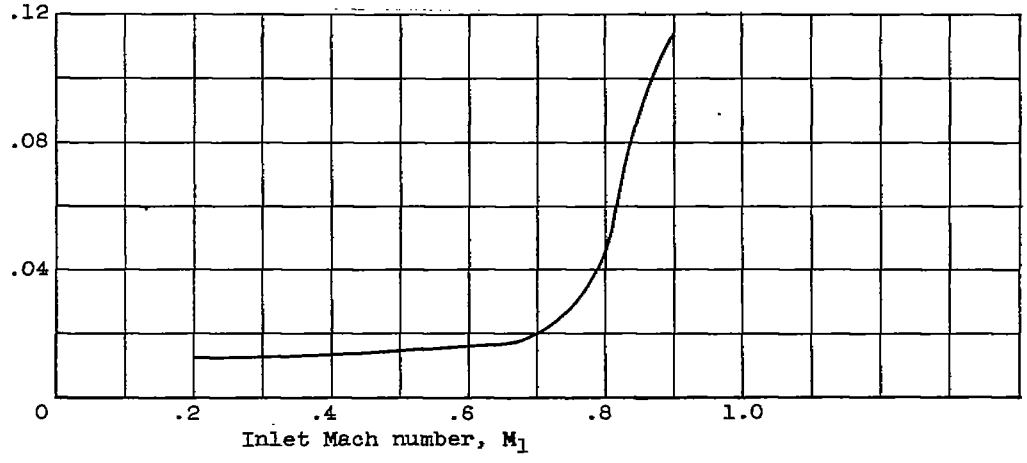

(b) Inlet Mach number for NACA 65-(12)10 blade. Solidity, 1.0; inlet-air angle, 45° (ref. 11).

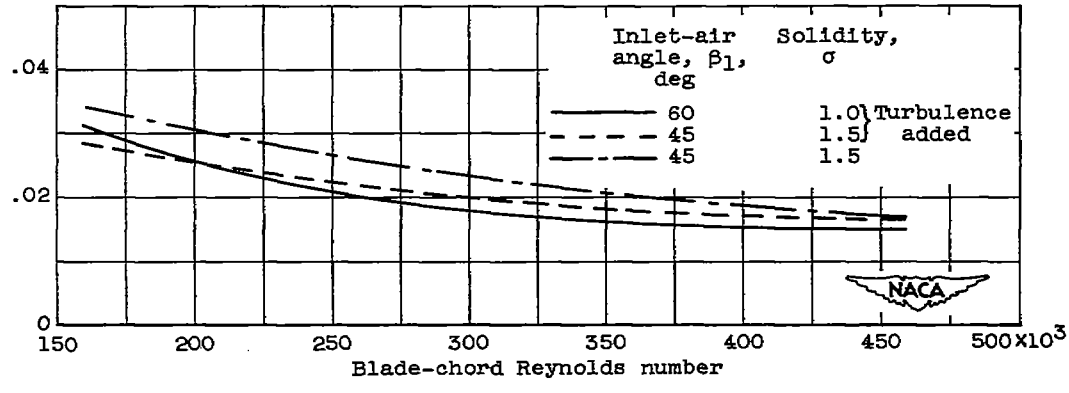

(c) Reynolds number for 65-(12)10 blade (ref. 3).

Figure 4. - Variation of blade-element total-pressure loss coefficient with various factors for NACA 65-series compressor blade sections in two-dimensional cascade at subcritical diffusion factors and at design angle of attack.

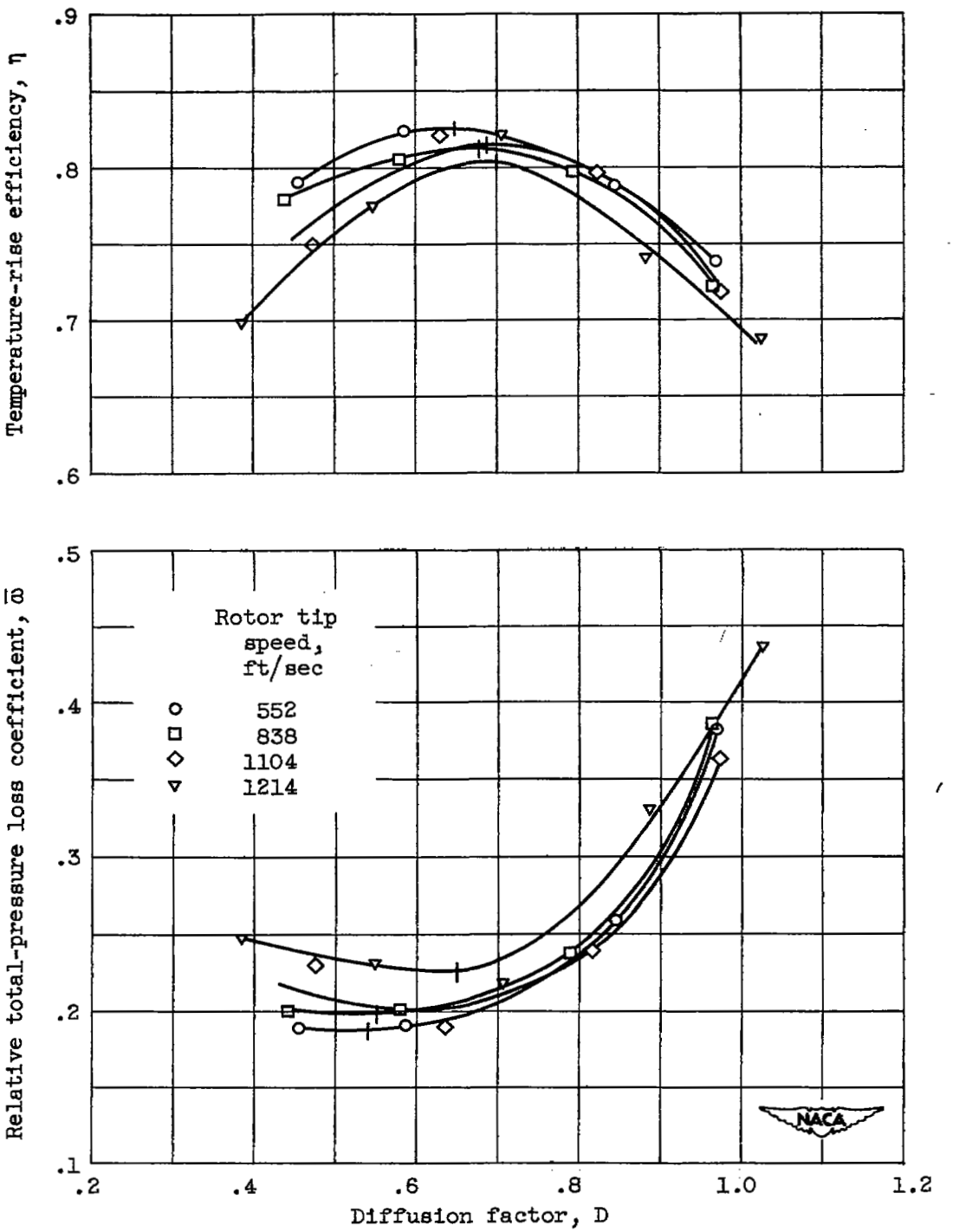

Figure 5. - Example of variation of blade-element temperature-rise efficiency and relative total-pressure loss coefficient with diffusion factor in tip region of rotor (rotor 9). Bars indicate minimum or maximum values.

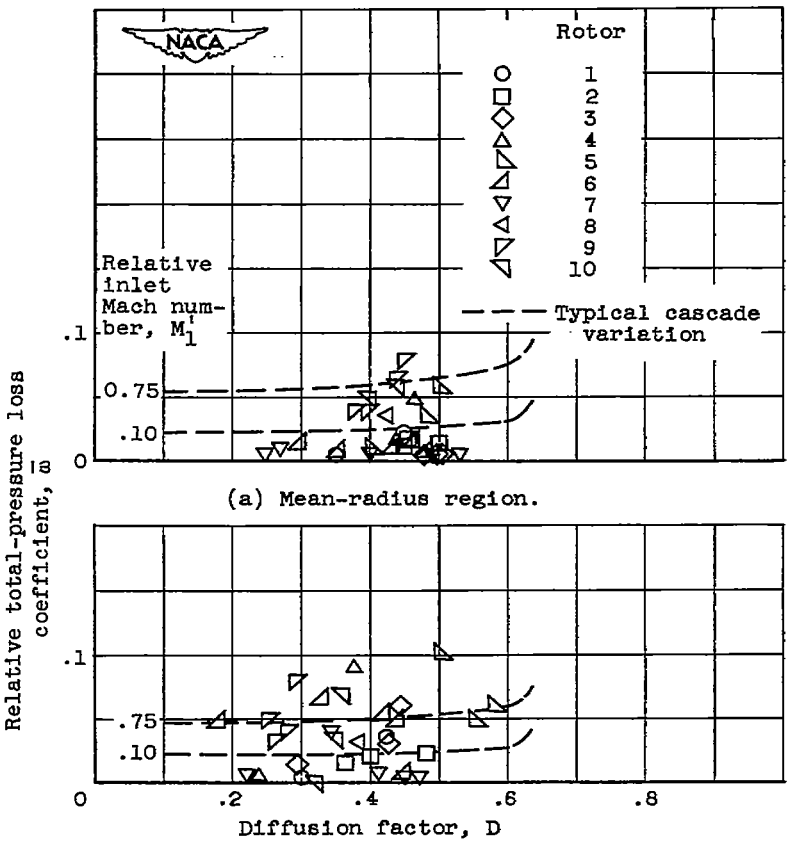

(a) Mean-radius region.

(b) Hub-radius region.

Figure 6. - Variation of minimum (design) blade-element relative total-pressure loss coefficient with diffusion factor for axial-flow single-stage rotors.

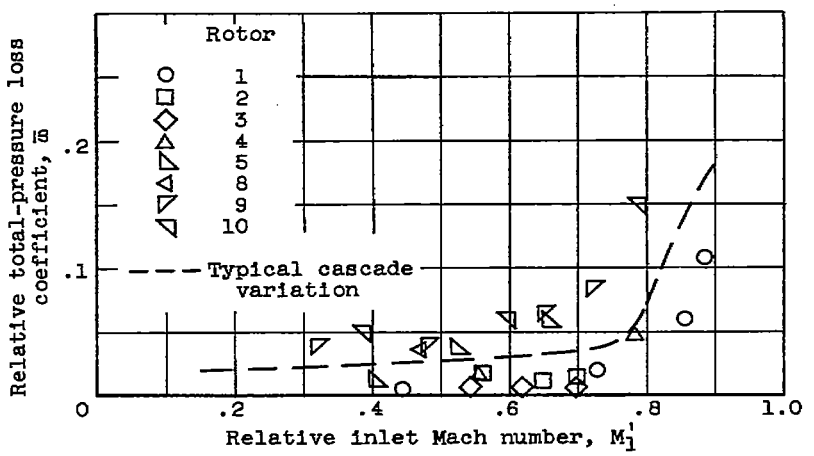

Figure 7. - Variation of minimum (design) blade-element relative total-pressure loss coefficient with relative inlet Mach number at mean radius for 65-series rotor blades.

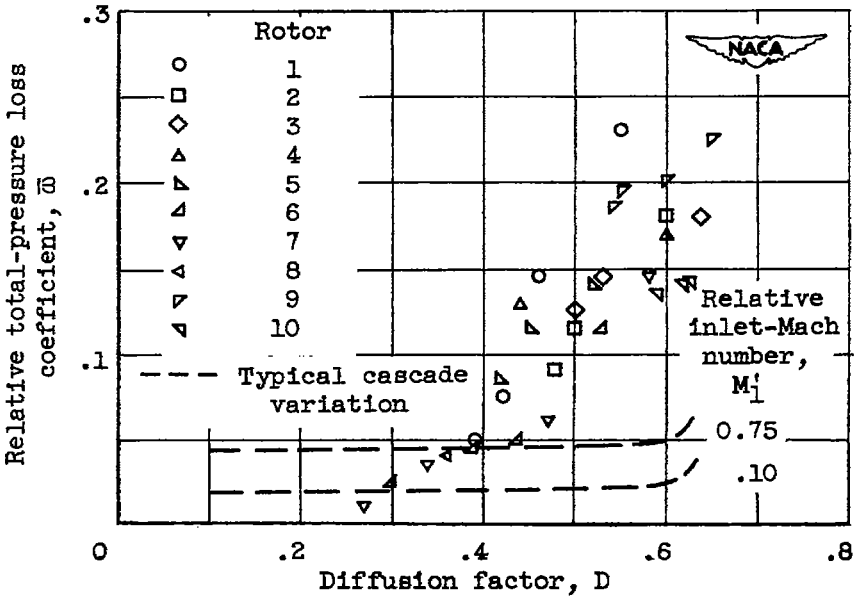

Figure 8. - Variation of minimum (design) blade-element relative total-pressure loss coefficient with diffusion factor in tip region of axial-flow single-stage rotors.

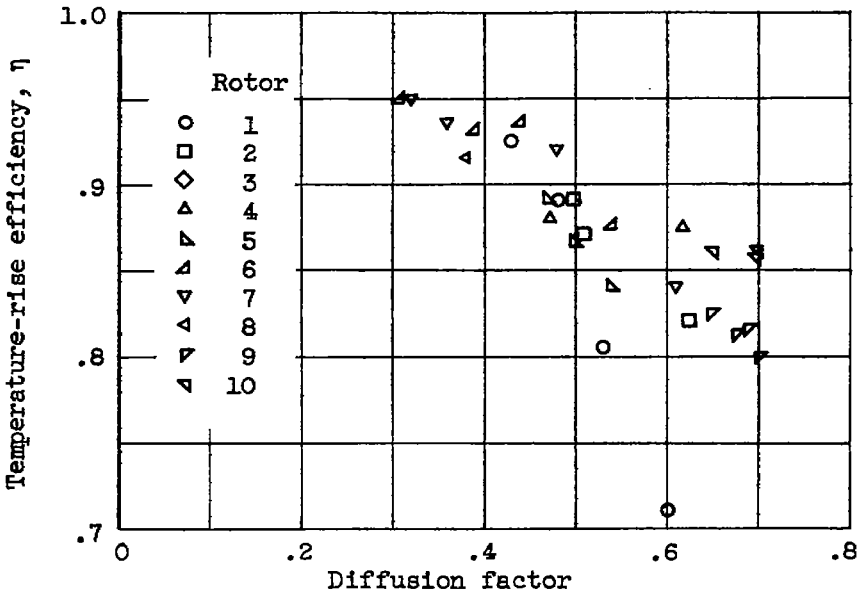

Figure 9. - Variation of maximum blade-element temperature-rise efficiency with diffusion factor in tip region of axial-flow single-stage rotors.

[redacted]

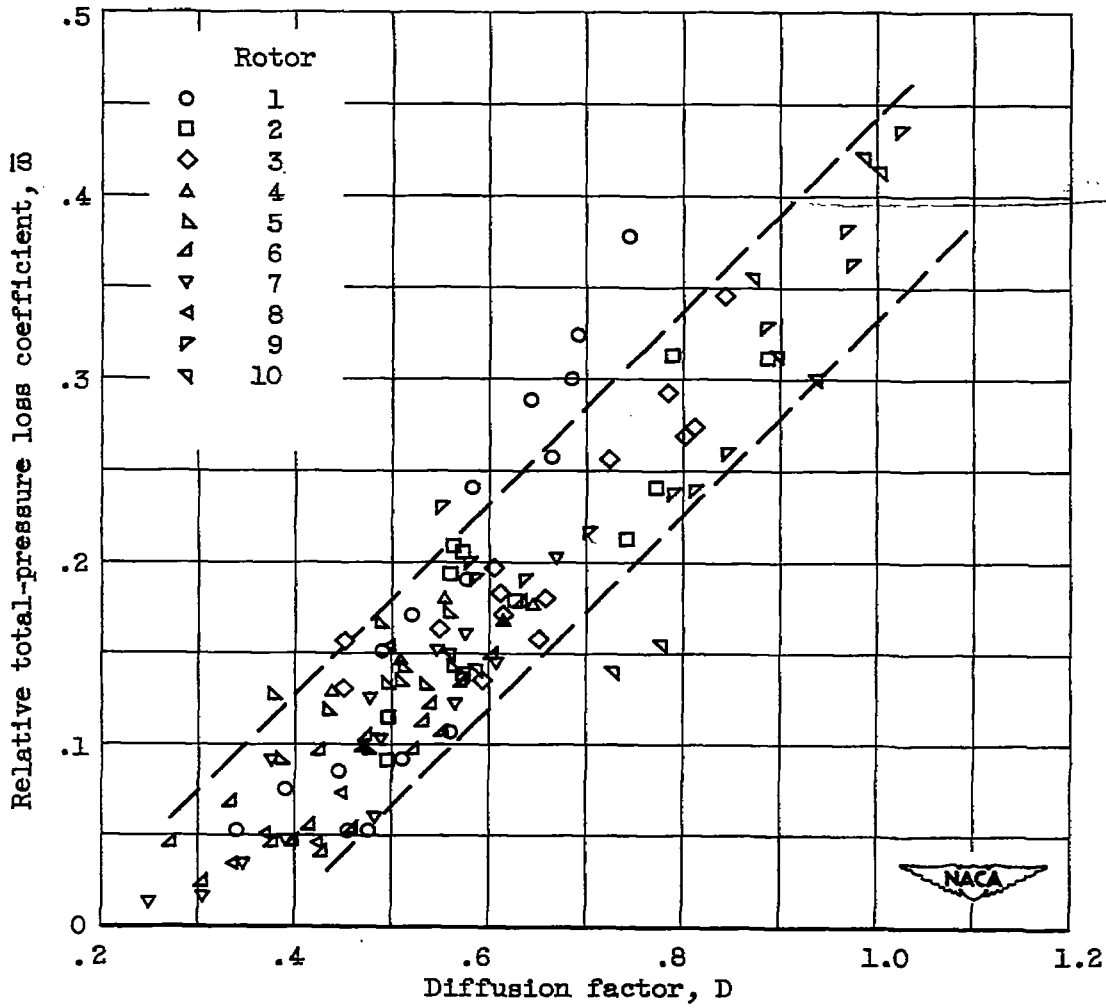

Figure 10. - Variation of blade-element relative total-pressure loss coefficient with diffusion factor in tip region of axial-flow single-stage rotors. All data points in positive incidence range from region of minimum loss to region of drop in efficiency of about 0.10.

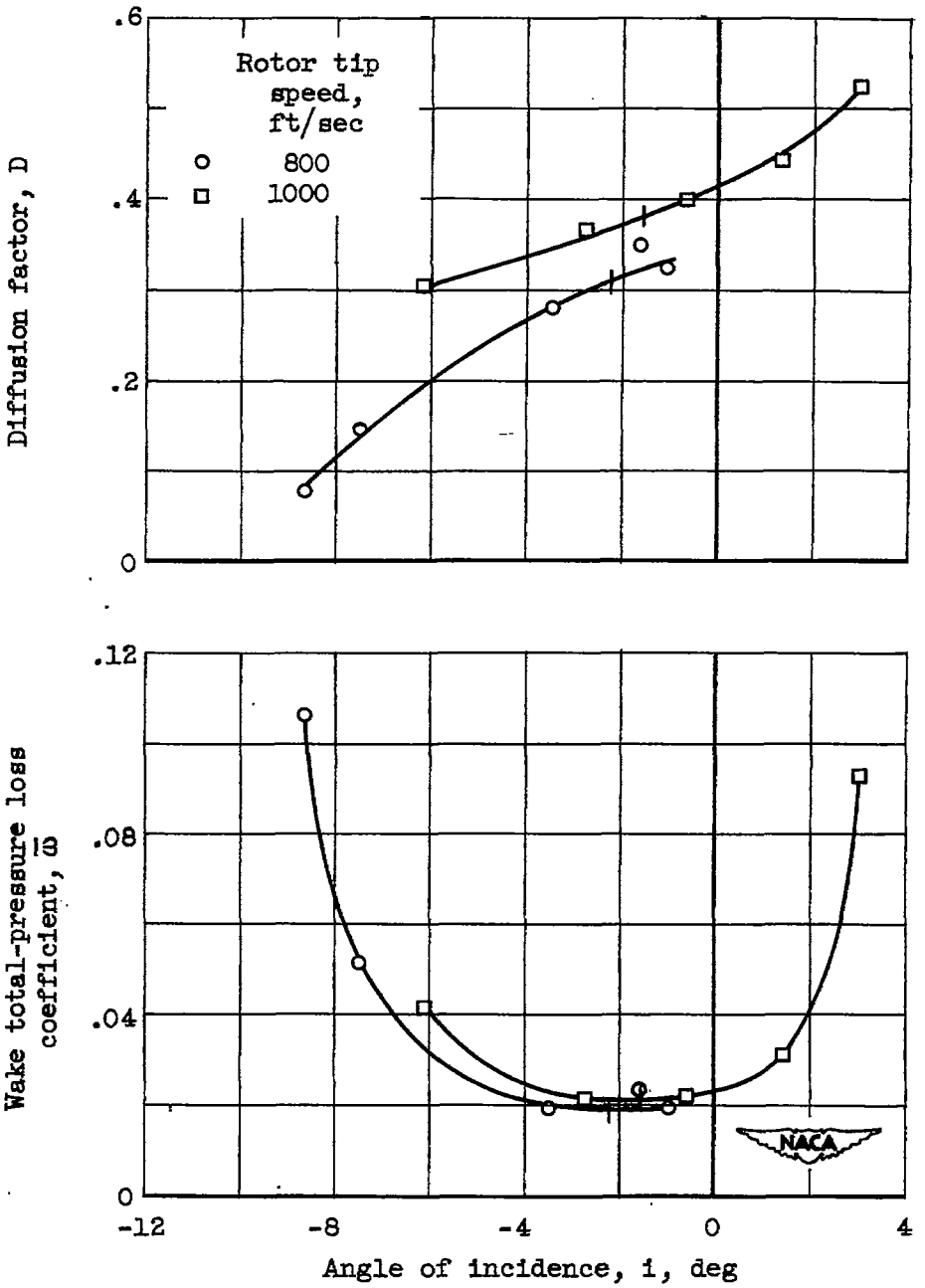

Figure 11. - Example of variation of wake total-pressure loss coefficient and diffusion factor with angle of incidence in hub region of stator (stator 1). Bars indicate points of minimum loss.

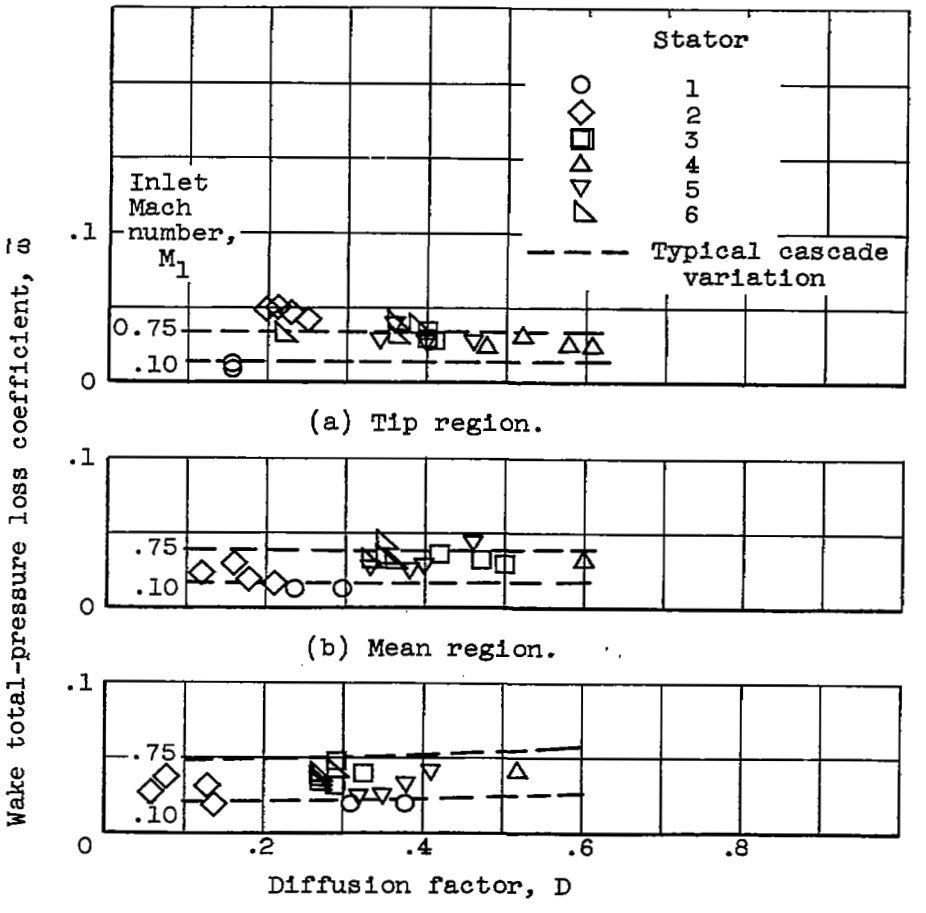

Figure 12. - Variation of minimum wake total-pressure loss coefficient with diffusion factor for axial-flow compressor inlet-stage stators.

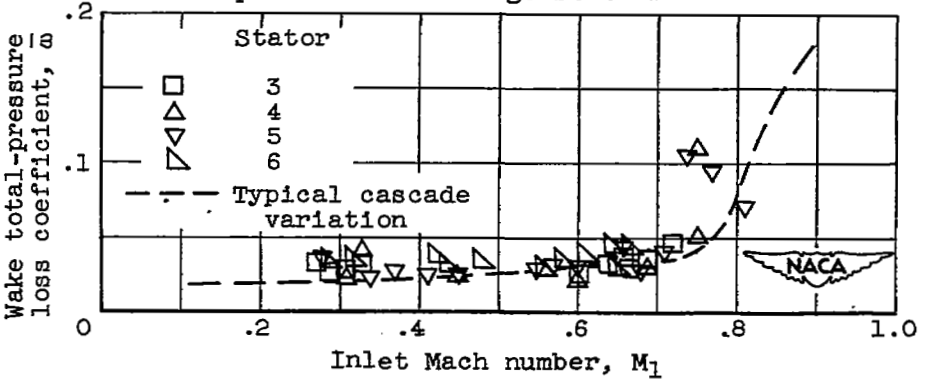

Figure 13. - Variation of minimum wake total-pressure loss coefficient with inlet Mach number at hub, mean, and tip regions of stators with 65-series profiles.

[redacted]